Flow Electrification Measurements of Transformer Insulation using a Couette Flow Facility

A. P. Washabaugh,

Raychem Corp., Menlo Park, CA

M. Zahn

Laboratory for Electromagnetic and Electronic Systems,
Massachusetts Institute of Technology, Cambridge, MA

ABSTRACT

A rotating cylindrical electrode apparatus, which provided cylindrical Couette flow, was used to simulate flow electrification in an electric power transformer. The apparatus had Shell Diala A transformer oil filling the annulus between coaxial cylindrical stainless steel electrodes that were either bare metal, or covered by a thin copper sheet and/or EHV-Weidmann HiVal pressboard insulation. Extensive experiments characterized the time transient and steady state behavior of the electrification through measurements of the volume charge density, the terminal voltage, and the terminal current as the system was driven out of equilibrium by changes in the flow rate (inner cylinder rotation rates of 100 to 1400 rpm, Reynolds numbers of 5×10^3 to 5×10^5), temperature (15 to 70°C), insulation moisture content (0.5 to 20 ppm in the oil), applied voltage (0 to 2 kV dc), and concentration of the non-ionizable antistatic additive 1,2,3 benzotriazole (BTA, 0 to 60 ppm). Generally, the electrification increased with flow rate and temperature but the BTA appeared to cause competing effects: it decreased the volume charge density on the liquid side of the interface by a factor of 4, which reduces the electrification, but also decreased the oil conductivity by a factor of 10, which enhances the electrification. A critical oil BTA concentration of 5 to 8 ppm minimized the electrification. The volume charge density was sensitive to the current flowing through the interface and surface charge accumulation. With pressboard covering the cylinders, the electrification effects of the temperature and moisture were decoupled during the transient following step reductions in the temperature. The oil moisture content did not affect the oil conductivity significantly, but the volume charge density varied inversely with the moisture content during an initial equilibration period just after the oil had been added to the system. The highest electrification was observed during this equilibration period.

1. INTRODUCTION

FUNDAMENTAL to any description of flow electrification is the charge transfer process that occurs at the interface between the liquid and the solid phases. In essence, it is the preferential adsorption (or difference in interfacial reaction rates) of one of the charged species that leads to the generation of the electrical double layer and it is the diffuse charge in the electrical double layer that is transported by the fluid to accumulate or leak away at a downstream location. Consequently, in order to develop a comprehensive understanding of flow electrification, it is important to characterize the solid/liquid interface. As an example, one

technique for studying interfacial charge transfer processes, developed in the field of electrochemistry, is to measure the current that flows between a stationary electrode and a rotating disk electrode [1] or a rotating cylindrical electrode [2, 3]. This terminal current can be related to parameters that describe the chemical reaction, such as rate constants, if the reacting species and the fluid flow profile are known.

Experiments with rotating electrodes are advantageous over stationary electrode or pipe flow experiments because they allow the kinetic processes at the electrodes to be studied under steady state and fully developed flow conditions. The rotating

electrode imposes a fluid flow profile that dominates the convection caused by the motion of the individual charged species in an electric field. For rotating disks, the fluid flow is stable up to high Reynolds numbers and laminar flow conditions are generally studied. In contrast, for rotating cylinders, the flow becomes unstable at low Reynolds numbers and turbulent flow conditions are usually studied. In electrochemistry, aqueous electrolytic solutions having well-defined ionic species are usually treated. With the electrode material also known, the oxidation-reduction reaction that occurs at the interface can then be formulated. This chemical reaction describing the interfacial mass and charge transfer, coupled with the equations that describe the transport of the reacting species to the interface, can then be related to the terminal current [2].

The rotating electrode technique for studying interfacial kinetics in electrolytic solutions has been used also to study the charge separation process of flow electrification in non-aqueous semi-insulating liquids [4–12]. While many of the fundamental concepts apply to both aqueous and non-aqueous systems, there are two significant differences. First, aqueous liquids tend to be much more conducting than the semi-insulating hydrocarbon liquids being considered here. This increased conductivity in aqueous liquids leads to increased charge relaxation so that the net charge density in the bulk of the fluid flow is near zero and interfacial properties must be inferred from terminal current measurements. For the semi-insulating liquids used in electric power apparatus, the net charge density in the bulk region of the fluid flow, the terminal current, and the terminal voltage can be measured and related to the interfacial properties [4, 13, 14]. Second, while the identity of the ionic species are usually known apriori in aqueous solutions, the ionized species of interest in flow electrification problems with insulating liquids are usually formed by trace impurities. The unknown composition of these trace impurities leads to inherent difficulties in creating reproducible measurements; one way to account for this complication is to use experimental materials that are the same as those typically used in electric power apparatus.

This paper describes an experimental investigation of flow electrification in a rotating cylindrical electrode system in which the effects of various parameters, such as temperature, moisture concentration, oil conductivity, terminal constraints, energization and additive concentration, are explored. While this work is primarily based upon an experimental apparatus that has previously been described [4, 7], it also introduces some newly developed sensors and methodologies. To put these results in perspective, comparisons are also made to rotating cylindrical electrode measurements in aqueous electrochemical systems.

2. EXPERIMENTAL APPARATUS

To simulate the flow electrification processes in a transformer and to study the effects that the oil and pressboard properties, such as moisture content, conductivity, and temperature, have on

these processes, a Couette experimental facility (CF) was developed. The CF had Shell Diala A transformer oil filling the annulus between coaxial cylindrical electrodes that were bare metal (stainless steel in this work) or covered with sleeves of other materials, such as copper and/or pressboard insulation. The inner cylinder could rotate at speeds giving controlled turbulent flow so that electric charge was transported from the electrical double layers at the solid/liquid interfaces to the volume of the fluid and the mass transfer of moisture between the oil and the pressboard was enhanced. By measuring the charge density in the liquid, the voltage across the cylinders and the current flowing between the cylinders, the electrification processes under various operating conditions could be studied. Similarly, by measuring the moisture in the oil as the operating conditions are changed, the mass transfer dynamics between the oil and the pressboard could be studied.

The CF, as shown in Figure 1, essentially consisted of a Couette charger (CC), which contained the rotating cylindrical electrodes, and a reservoir for storing the oil [4, 7]. The CC and the reservoir were equipped with heating tape and a cooling coil such that the temperature was controlled from 15 to 100°C. The reservoir could hold 11.4 l while the CC could contain 7.5 l. In this facility, the inner cylinder had a radius of 7.62 cm, the outer cylinder had a radius of 10.16 cm, and the cylinders had a height of 0.4 m. For these experiments, the outer stainless steel cylinder was always kept bare and was used as a reference electrode. This helped make the temperature through the CC more uniform and avoided complications in interpreting moisture measurements since the mass transfer dynamics only occurred at the inner pressboard cylinder. Experiments were performed with the bare stainless steel inner cylinder, with a sheet of 0.254 mm copper epoxied to the inner cylinder, and with 1 mm thick EHV-Weidmann HiVal™ pressboard insulation epoxied to either the inner cylinder or the copper sheet. To create a measurable volume charge density inside the oil, the inner cylinder was rotated at angular rotation rates up to 2000 rpm. For transformer oil, rotation rates $\gtrsim$ 60 rpm leads to turbulent flow in the oil-filled gap between the cylinders [7]. In turn, the mixing due to the turbulent flow led to a region of essentially uniform charge density which could then be measured.

Before each experiment, with and without pressboard, the system was vacuum processed to the dry conditions found in actual transformers by pulling a vacuum and raising the temperature. The drying time was based on previous experience in drying the pressboard. Typically, the CC with not oil-impregnated pressboard was kept at a pressure of 13 to 33 Pa and a temperature of 90°C for 1 to 14 days while the oil-filled reservoir was kept at 13 Pa and 70°C for 1 to 12 h. After the drying process was completed, the pressboard was oil impregnated by transferring oil from the reservoir into the CC.

The charge density in the oil between the cylinders was measured using an absolute charge sensor (ACS), which brings a sample of fluid from the turbulent core of the CC into a Faraday cage [14]. The ACS sampling probe was mounted so that its end was flush with the edge of the outer cylinder that was in contact with
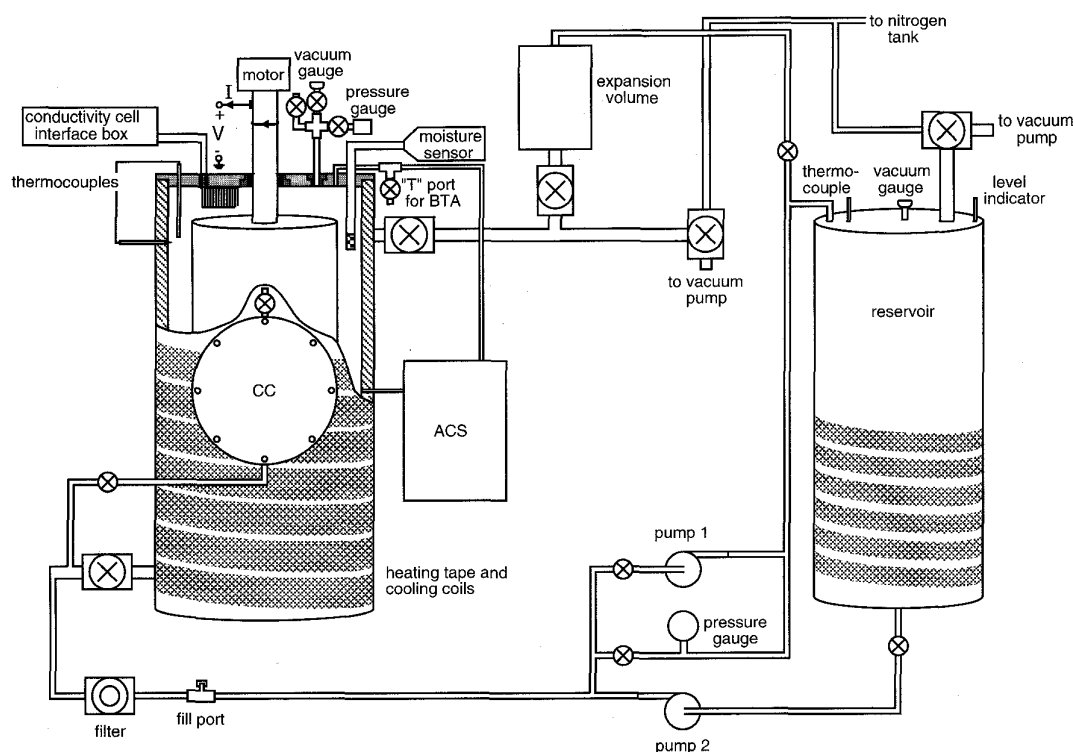
Figure 1. The Couette facility, where rotation of the inner cylinder creates controlled turbulent flow. An absolute charge sensor (ACS) was used to measure the charge density in the oil region between the coaxial cylinders of the Couette charger (CC). A moisture sensor was placed in the oil gap between the cylinders. A conductivity sensor was mounted above the inner cylinder. The expansion volume and the reservoir were used to allow the oil to expand and contract as the temperature of the CC varied.

the oil (within 1 mm). In this position, the sampling probe should have had a minimal effect on the electrification process being studied. A data acquisition program was used to take the measurements and periodically set the rotation rate of the inner cylinder. Typically, an entire set of measurements took ∼ 3 min, with most of the time spent on the charge density and conductivity measurements.

The conductivity of the oil was measured with a ganged parallel plate capacitor that was mounted in the oil space above the inner cylinder. This conductivity sensor had one set of plates driven at a 1 V peak, 0.1 Hz ac voltage, while the other set of plates, the sensing electrodes, measured a signal that is attenuated and phase delayed with respect to the driven signal. The measured signals depend upon the permittivity and conductivity of the oil and were used in a parameter estimation routine to calculate the oil conductivity [15]. A grounded stainless steel mesh surrounded the plates to act as a shield and to reduce the flow rate of the oil between the plates, thereby reducing electrification along the plates themselves. The mesh size was on the order of 1 mm so oil was also able to circulate through the sensor. The capacitance between the shield and the sensing plates was not significant in these measurements.

The oil moisture content was measured using two techniques. The first technique was to withdraw samples of oil occasionally from the CC and to measure the moisture content with a

Mitsubishi CA-05 moisture meter (MM), which performs a Karl-Fisher titration. This technique is accurate for moisture contents > 1 to 2 ppm. Since one of the goals of this research was to understand the electrification process at low temperatures where the moisture levels can be < 1 ppm, another method for measuring the moisture was required. The second technique was to monitor the moisture level in the oil continuously, using newly developed polyimide-based capacitive humidity sensors [16, 17]. These experiments used a Harley moisture sensor CT-880-BN-H (0/100%)-X instrument, with the sensor itself placed in the gap between the cylinders.

In order to use these moisture sensors to determine the absolute moisture content, the oil temperature had to be known accurately. Furthermore, the equilibrium curves describing the partitioning of moisture between the oil and the pressboard are temperature dependent [18]. In these experiments, the temperature of the CC was measured in two different locations. The first location had a thermocouple probe passed through the top flange of the CC so that the oil temperature in the well-mixed flow region was measured. The second had a thermocouple probe passed through the side wall on the outer cylinder of the CC so that the probe tip penetrated ∼ 1 mm into the oil. This side location was sensitive to both the oil temperature near the wall and the temperature of the outer cylinder. Significant thermal gradients (> 10°C) were observed while attempting to maintain the system at temperatures

below ambient with high rotation rates because the heat caused by the viscous shear of the rotating inner cylinder became appreciable, or during imposed temperature transients. To minimize the effects of these gradients, except during the imposed temperature transients, the experiments were performed at rotation rates and temperatures where both temperatures were approximately equal to within $\sim 3°C$.

The terminal voltage and short-circuit current were measured using a Keithley 617 electrometer. In some cases, dc voltages were applied across the cylinders. These voltages were initially set manually with a Hewlett Packard 6218 C power supply, but later measurements had the capability of controlling the voltage built into the data acquisition software. When set automatically, the voltage was generated by a Wavetek arbitrary waveform generator, model 75, and amplified by either a Trek 20/20 HV Amplifier or a Heathkit HV operational amplifier, model EUW-19 A.

In several experiments, the additive 1,2,3 benzotriazole (BTA) was added to the CC to determine its effects on the electrification processes. The procedure for adding the BTA to the oil was to have the CC operating at an elevated temperature first (such as 70°C), then a concentrated solution of BTA in oil (such as 300 ppm weight BTA/weight oil), which was prepared in a beaker at elevated temperatures outside the CF, was added to the CC through a 'T' connection where the ACS discharge line returned to the CC, as shown in Figure 1. Since the CC contained ≈ 7.5 l of oil (6.75 kg using a mass density of 0.9 g/ml) only ~ 125 ml of the concentrated solution had to be added to raise the average BTA concentration 5 ppm. To monitor the BTA content of the oil, samples of oil were withdrawn from the CC and the BTA concentration measured by ultraviolet spectrophotometry [15]. Although the same port of the CC was used for both adding and withdrawing the BTA filled oil, the discharge from the ACS circulated the oil from the 'T' into the CC and the sampling line was always flushed with oil from the CC before a sample was withdrawn.

3. REPRESENTATIVE RESULTS

Several types of representative measurements are presented in this Section. The general approach was to measure the baseline response for the system with bare metal cylinders and with HiVal pressboard covering the inner cylinder. Then the effects of adding copper, which is present in large quantities in transformers, and the additive BTA were explored. In each case, the controllable parameters (inner cylinder rotation rate, temperature, and applied dc voltage) were varied as the measurable quantities (charge density, terminal current or voltage, oil moisture content, oil conductivity, and pressboard conductivity) were monitored. When possible, both steady state and transient conditions were explored.

The approach used for these experiments was self-critical with the measurements occasionally being repeated up to 20 or 30 times for a given set of conditions. To check reproducibility, measurements were taken for both increasing and decreasing rotation rates and temperatures. To further check the reproducibility, the oil and/or the pressboard in the system were periodically replaced. Although aspects of the data were quite reproducible,

such as an increase in the charge density with rotation rate, some of the details of transient measurements were not reproducible. Whenever possible, representative measurements from numerous experiments are provided.

In this paper, the basic data from the experiments are plotted. While it is natural to express the measured quantities in terms of nondimensional parameters, such as the hydrodynamic Reynolds number, most of the interdependencies of the various quantities are not known so it is more convenient to express the data in dimensional form. An exception is Section 4, where normalizations motivated by the electrification models and the electrochemistry literature are presented. Subsequent papers will develop electrification models and present the data in a nondimensional form.

3.1. ROTATION RATE DEPENDENCE

The obvious variable parameter that is critical to flow electrification is the fluid flow rate. In the CC, the flow rate was controlled by the rotation rate of the inner cylinder. Physically, as the rotation rate increased, the flow rate also increased but the diffusion sublayer thickness (the thickness of the interfacial region where the effective diffusivity from the turbulence is dominated by molecular diffusion) decreased. The net result was that the core charge density tended to increase with rotation rate as the sublayer thickness decreased, and more charge was transported by convection, out of the interfacial electrical double layers into the core region of the flow.

Sample sets of steady state electrification data are shown in Figure 2 for identical bare stainless steel cylinders and in Figure 3 for pressboard insulation covering a copper layer on the inner cylinder. For the bare cylinders, the charge density had the same polarity as the terminal current and voltage at high rotation rates, but the opposite polarities at low rotation rates. As shown in Figure 1, the electrometer measured the terminal voltage and current in the external circuit from the inner cylinder to the grounded outer cylinder. In contrast, when pressboard insulation covered the inner cylinder, the charge density had a polarity opposite that of the terminal current and voltage for all rotation rates. Also significant about these data is that the measured quantities tended to increase in magnitude as the rotation rate increased and did not reach a limiting or saturation value. This indicates that the interfacial charge transfer process was probably rate limited by the transport of ionic species to the interface, not the interfacial reaction rate.

The polarity reversal of the terminal quantities as the rotation rate increased is shown more clearly in Figure 4. As the rotation rate was varied, either the short-circuit current or the open-circuit voltage was monitored. The current was measured during both the startup and shutdown transients for the rotation of the inner cylinder. For the voltage measurements, the voltage was initially set to zero (short-circuited) until the inner cylinder reached a steady state and then the terminals were open-circuited as the voltage transient was measured. Afterwards, the decaying voltage transient was measured when the cylinder stopped rotating. In one case (at 1000 rpm) the electrometer was zeroed
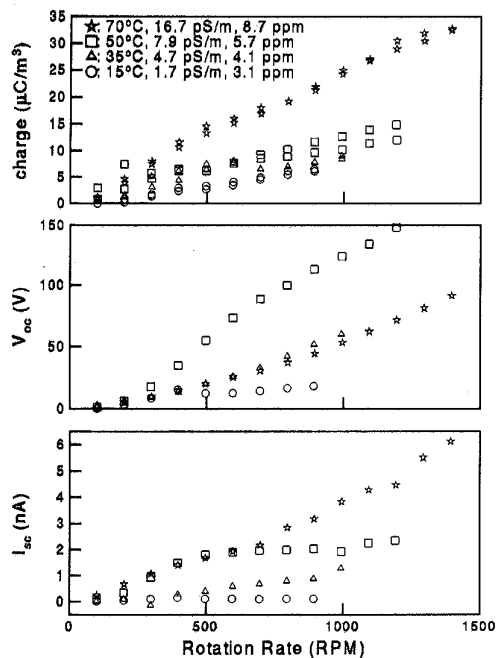
Figure 2. Electrification for bare stainless steel cylinders. The charge density, open-circuit voltage and short-circuit current usually had the same polarity and increased with rotation rate. At each temperature and rotation rate, the open-circuit and short-circuit charge densities are plotted and appear to be essentially the same. The maximum voltage for each rotation rate appeared at an intermediate temperature (50°C).

Figure 3. Electrification for HiVal pressboard covering a copper sleeve on the inner cylinder. At each temperature and rotation rate, the open-circuit and short-circuit charge densities are plotted and appear to be essentially the same. The charge density had a polarity opposite that of the terminal voltage and current.

during the open-circuit measurement and the transient associated with the voltage rising to its steady state level was repeated. The rapid increase in current as the rotation was started was probably due to the redistribution of charge in the oil by the turbulent mixing. Similarly, during the shutdown transient, some of the response can be attributed to the relaxation of the charge in the bulk of the oil, but it also took a few seconds (usually 10) for the inner cylinder to stop rotating and the oil to come to rest. Similar measurements were obtained at other temperatures [15]. Although the charge density was not monitored because the sampling time for the ACS was long compared to the duration of the transients, the steady state charge density and short-circuit current were measured immediately prior to the transient measurements and showed that the charge density always remained positive [15]. Subsequent papers develop a model which describe this behavior in terms of the wall charge densities on the liquid sides of the solid/liquid interfaces. Assuming that the wall charge densities are positive, with the outer cylinder charge density slightly larger than the inner cylinder's, the measured charge density is also positive but the terminal voltage (created by the difference in wall charge densities and the cylindrical symmetry) changes polarity as the flow rate increases and relatively more charge is transported away from the inner cylinder interface.

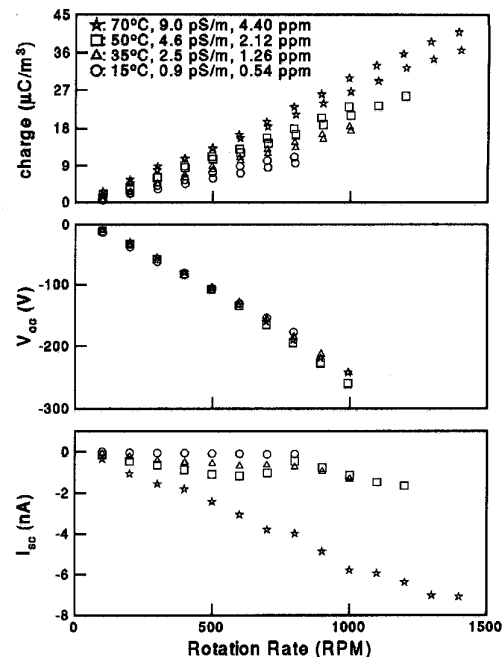The transient associated with step changes in the rotational

speed also provides some insight into the electrification processes. While the development time for the fluid mechanics to reach a steady state is on the order of $\sim$ 3 s, the time necessary for the electrical variables to reach a steady state depends upon the terminal connections. With the terminals open-circuited, no current flows through the external circuit and the charge density and voltage reach a steady state with the dielectric relaxation time of the oil ($\sim$ 1 to 20 s) as the time constant. Since the sampling time between the experimental measurements was typically longer than the oil relaxation time, the charge density and voltage changed with the rotation rate, as shown in Figure 5 for pressboard insulation covering the inner cylinder. Note that this development time was independent of the pressboard dielectric properties because there was no net current flow. When leakage currents flowed through the pressboard, for example through a relatively low impedance path between the grounded conductivity cell shield and the top of the inner cylinder, a significant field developed inside the pressboard with the relaxation time of the pressboard as the time constant [15, 19]. To minimize the effect of the pressboard field gradually increasing, the conductivity cell was disconnected and the experiments had a relatively short duration during open-circuit measurements.

In contrast with the open-circuit measurements, when the terminals are short-circuited the time constant for reaching steady state depends intimately upon the pressboard dielectric properties. While the charge density still attained a steady state quickly as the rotation rate was changed, as shown in Figure 6, the terminal current changed abruptly and then slowly approached
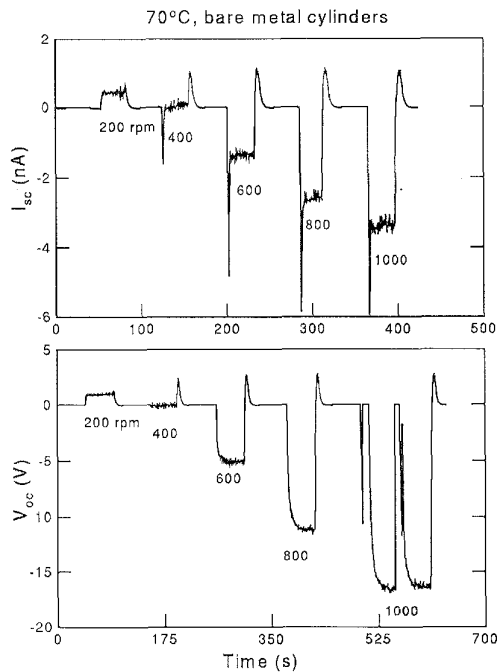
Figure 4. Time transient terminal measurements with bare stainless steel cylinders for various inner cylinder rotational speeds. The current and voltage were set to zero (by open or short-circuiting the electrometer) as the rotation rate (in rpm) was set. Note the polarity reversal between low and high rotation rates.
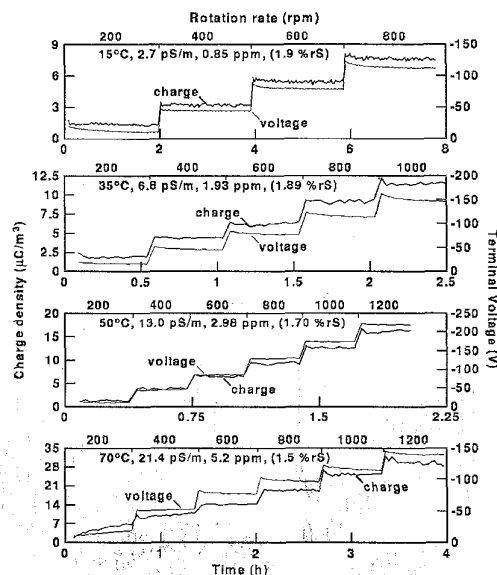

Figure 5. Transient open-circuit voltage and charge density measurements for HiVal pressboard covering the inner cylinder. The open-circuit voltage and charge density follow step changes in the rotation rate.

its steady state level. Since the charge density remained essentially constant over this period, the redistribution of charge and the volume charge densities on the liquid side of the interfaces were independent of the current flowing through the system.
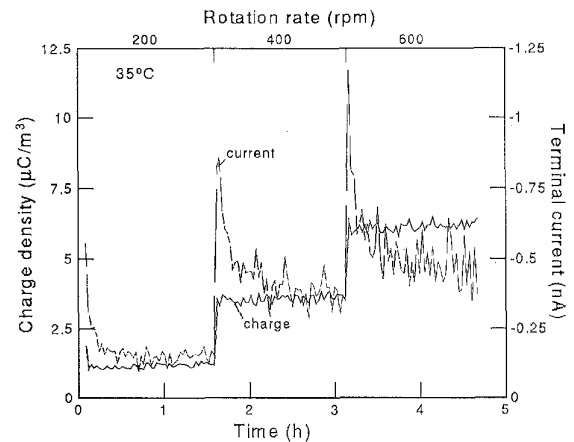

Figure 6. Transient short-circuit current and charge density measurements using the same materials as in Figure 5, with HiVal pressboard covering the inner cylinder. While both the charge density and the current change with the rotation rate, the current slowly approached its steady state level as surface charge accumulated at the interface between the pressboard and the oil.

This is consistent with the accumulation of surface charge at the oil/pressboard interface. Furthermore, this accumulated surface charge leads to a field inside the pressboard, not in the oil, because the oil volume charge density remains constant.

3.2. TEMPERATURE DEPENDENCE

The system temperature is readily controlled but the temperature dependent material properties (viscosity, conductivity, relative moisture content between the oil and the pressboard, ion mobility and diffusivity, and the interfacial zeta potentials creating the electrical double layers) can lead to competing effects. For example, the viscosity of the oil decreases as the temperature increases. This causes the diffusion sublayer thickness to decrease and more charge to be carried out of the electrical double layers into the bulk of the fluid. In contrast, the conductivity increases with temperature, which results in an increase in charge relaxation and a decrease in the volume charge density.

Sample sets of steady state electrification data showing the variations with temperature are given in Figures 2 and 3. In both sets of data, the charge density and short-circuit current increased with temperature at each rotational speed, to within the accuracy of the measurement. In contrast, the open-circuit voltage was largest at an intermediate temperature (near 50°C) for the bare metal cylinders but essentially independent of the temperature when pressboard covered the inner cylinder. Although these pressboard measurements had a copper sleeve over the inner cylinder, measurements without the copper sleeve present gave similar results.

During temperature transients, the short-circuit current, charge density, moisture, and conductivity usually increased in magnitude with the temperature, as shown in Figure 7 for a step increase in temperature and in Figure 8 for some temperature cycling. The charge density and current also showed long time scale
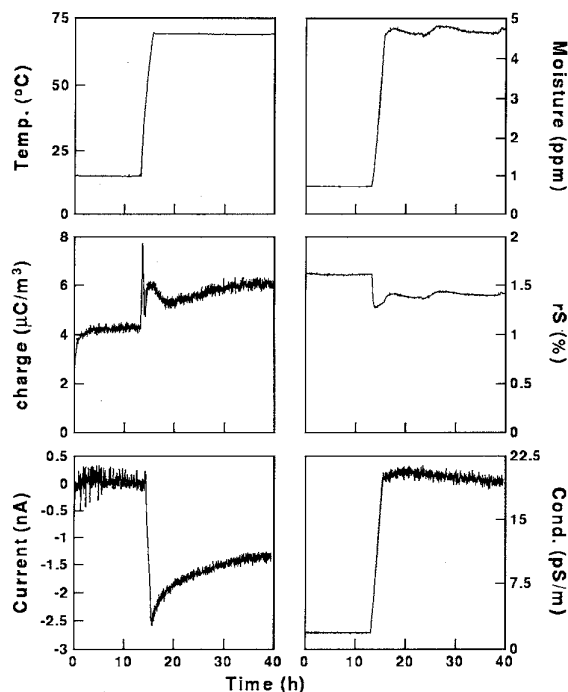
Figure 7. Temperature driven transient measurements at 400 rpm for HiVal pressboard covering the inner cylinder. The oil moisture content and conductivity followed the temperature, indicating a relatively rapid mass transfer of moisture from the pressboard into the oil at elevated temperatures. The current and charge density became larger as the temperature increased.

transients after the temperature stabilized. While the accumulation of surface charge at the pressboard/oil interface was too short at the elevated temperatures to describe this transient, it is possible that the properties of the pressboard itself were changing. The data in Figure 7 show the response of the first temperature increase in the system after oil impregnating the pressboard. By measuring the voltage decay after applying a battery to the stationary inner cylinder, the effective conductivity of the pressboard decreased after the initial low temperature electrification measurements [15]. The slow decrease in the terminal current at 70°C is consistent with a slowly decreasing pressboard conductivity. After a few days at the elevated temperature, the data of Figure 8 was taken. Since the current did not appear to change appreciably with time at 70°C, the pressboard conductivity apparently reached a steady state.

3.3. MOISTURE DEPENDENCE

One ubiquitous impurity present in both the solid and liquid insulation is water. Standard procedures for reducing the moisture content of the insulation include heating the system and vacuum processing, but some water is always present. In the steady state, the moisture equilibration curves show that the concentration of water in the hydrophilic pressboard is much higher than that of the hydrophobic oils. Unless the volume of oil is extremely large compared to the volume of pressboard, most of the water is
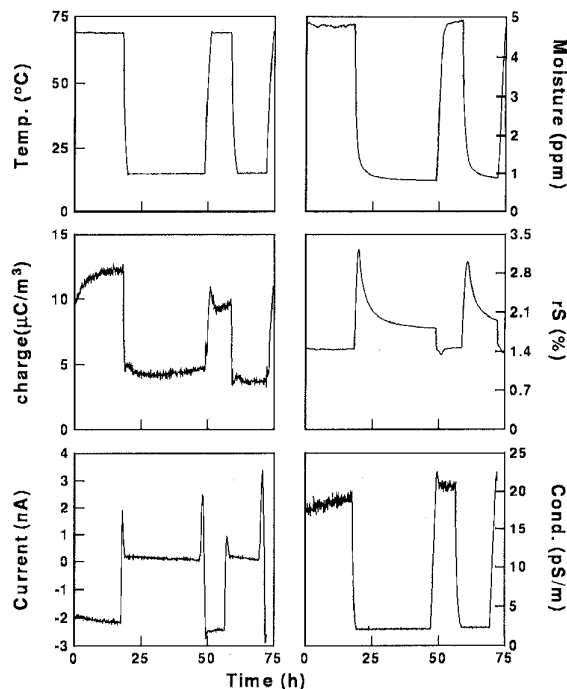

Figure 8. Temperature driven transients at 400 rpm for HiVal pressboard covering the inner cylinder. This data is a continuation of that given in Figure 7. The charge density decreased slightly with time as the oil became more conducting. The oil moisture content reached a steady state level quickly at 70°C but slowly at 15°C. Since the charge density quickly reached steady state at the low temperatures, the charge density appeared to be independent of the oil moisture content in this dry regime. The current usually followed the temperature, except during the transient in which the temperature was changed.

contained in the pressboard. In the CC, when the inner cylinder is covered with pressboard, the pressboard volume is $\sim$ 200 cm^3 while the oil volume is $\sim$ 7500 cm^3. Using mass densities of 1.0 g/cm^3 for the pressboard and 0.9 g/cm^3 for the oil, it is estimated that a 3 ppm (moisture weight/oil weight) change in oil moisture content only leads to an average change in the paper moisture content of 0.01%.

Moisture transients were induced by changing the temperature of the system, when the equilibrium pressboard and oil moisture contents changed. In Figure 9, moisture was transferred from the pressboard into the oil as the temperature was raised from 15 to 70°C. The moisture content followed the temperature and approached a steady state level of $\sim$ 7 ppm after the first temperature increase, but after additional vacuum processing, the oil moisture content no longer followed the temperature closely and slowly increased with time. This slow increase in moisture was probably not due to a leak to atmosphere since the 70°C oil conductivity slowly decreased, indicating a lack of oxygen for oxidation of the oil, and the absolute rate of increase of the moisture did not remain constant even though the relative humidity of the air was essentially constant. It was probably not due to the redistribution of moisture in the pressboard either because the initial
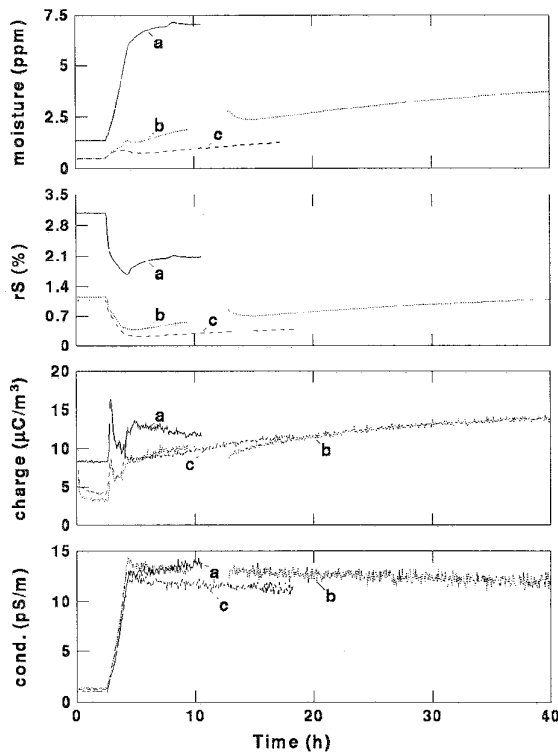
Figure 9. Temperature driven moisture transients at 400 rpm for HiVal pressboard covering the inner cylinder. The temperature was raised from 15°C to 70°C at time 2.5 h. The conductivity followed the temperature and then decreased slowly. With increased vacuum processing [initial case (a), then (b) and (c)] the oil moisture content decreased but it took longer to reach steady state levels at 70°C. The charge density increased with the temperature and appeared to be independent of the absolute oil moisture content.

experiment (case a) showed the moisture reaching a steady state quickly and a moisture dynamics model for the CC suggests that the mass transfer is rapid at elevated temperatures [17]. Rather, these data suggests that vacuum processing affects the manner in which water is held in the pressboard, such as decreasing the diffusivity of water in the pressboard, possibly through degradation of the cellulose fibers. This decreased diffusivity is consistent with the observations of Foss [20], in which the moisture concentration C (in percent) affected the diffusivity D according to

$$D = D_o \exp[0.5C] \tag{1}$$

with D_o a temperature dependent coefficient. Using the measured oil moisture content and the Norris curves relating the equilibrium concentrations of moisture in the oil and the paper, the pressboard moisture concentrations can be inferred [18]. For this experiment, the pressboard moisture content appeared to decrease from 0.74% in case (a) to 0.14% in case (c). The diffusivity in case (c) is then estimated to be 0.74× the diffusivity of case (a). While the decreased diffusivity does not appear to describe completely the long time transient moisture behavior, it is consistent with the measurement.

Figure 9 also shows that the charge density was not simply dependent on the absolute oil moisture content. While the largest charge densities were initially obtained with the wettest oil, comparable charge densities were also obtained at lower moisture contents after the initial vacuum processing. In contrast, although the oil conductivity also changed slightly, tended to increase with the moisture content in each case. Voltage decay measurements of the pressboard dielectric relaxation time at 70°C gave 108 s for case (a), 89 s for case (b) and 191 s for case (c), which suggests that the conduction through the bulk of the pressboard did not change appreciably throughout these measurements [21]. These observations implicate the 'conditioning' or past history of the system, not simply the oil moisture content, as having a critical role in determining the charge density.

3.4. OIL CONDUCTIVITY DEPENDENCE

Since the conductivity of the oil was not controlled by means of dissolving additives into the oil, the oil conductivity had a tendency to change with time. In some cases, the conductivity decreased, possibly indicating an adsorption of the trace impurities to the walls of the CC or even an absorption of the impurities into the pressboard insulation. There were also many situations in which the conductivity increased with time, possibly due to the oil being oxidized or the pressboard insulation released impurities into the oil.
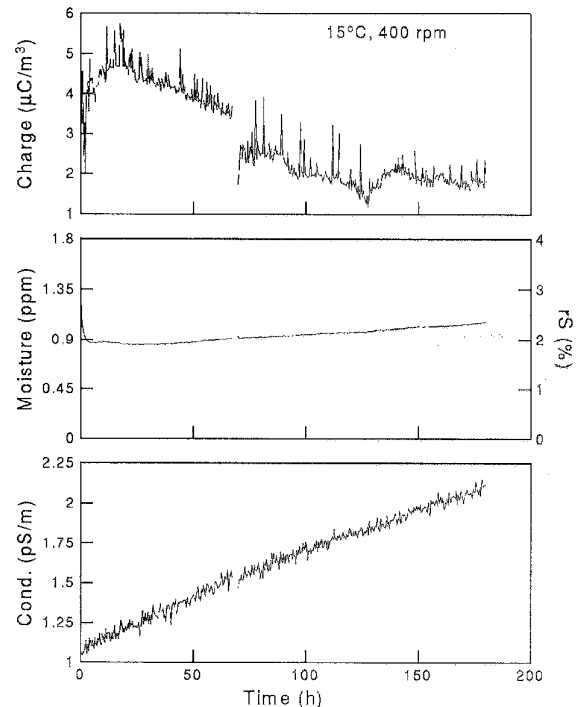

Figure 10. Oil conductivity effects on the charge density with HiVal pressboard covering the inner cylinder. The charge density tends to decrease with increasing conductivity. The gap in the data at time 65 h occurred when the data acquisition program was restarted.

The time variation of the oil conductivity was used to explore the charge density dependence on the conductivity when the other parameters such as the temperature and moisture content remained reasonably constant. One set of data that satisfied these criteria is shown in Figure 10. The oil moisture content initially decreased as the pressboard dried the oil because immediately prior to the measurement the system had been at 80°C and had a high oil moisture content. The moisture content then remained essentially constant, only increasing slightly, over the duration of this test. In contrast, the oil conductivity increased almost linearly with time. Except for an initial increase in charge density, possibly due to the accumulation of surface charge at the oil/pressboard interface, the charge density decreased almost linearly with time. The decreasing charge density with increasing conductivity is consistent with a 'constant wall charge density (ρ_w)' model in which the charge density goes as $\rho_o \approx \rho_w \tau_{oil}/\tau_d$, with τ_{oil} the oil dielectric relaxation time and τ_d the diffusion time across the interfacial diffusion sublayers [4, 7]. The data are consistent with pipe flow experiments showing an initial decrease in the charge density when the oil is aged, but the oil conductivity itself was not given [22].

3.5. APPLIED DC VOLTAGE DEPENDENCE

Many researchers have shown that the electrification charge density can be increased by HV ac energization [7, 23]. The applied field enhances the migration of charge across the diffusion sublayers which leads to an increase in the net charge density in the well-mixed core region of the flow. If the field is large enough, which is typically the case in electric power apparatus, charge can also be injected into the fluid. While this has practical application in electric power apparatus, it only provides limited information about the electrification processes since new parameters, such as an injection charge density [7], are also introduced to explain the phenomenon. In contrast, application of dc voltages causes net charge to develop on the interfaces in the system, similar to the separation and accumulation of charge inherent in the flow electrification processes. In this Section, some transient measurements with high dc voltages applied across the cylinders are presented, but the bulk of the measurements utilize relatively small dc voltages under steady state conditions.

Representative measurements of the charge density variation with small dc applied voltages are shown in Figure 11. The charge density increased linearly with the applied voltage in both cases. The resolution of the measurements is illustrated by the scatter in the data at each voltage. Even though the charge densities were quite small and near the resolution of the instrument, the linear variation in charge density was quite distinct. This linear dependence on the applied voltage does not appear to be an experimental artifact of the ACS since the offset current due to leakage current into the ACS was independent of the applied voltage.

Related measurements showed that the charge density had a slight dependence on the terminal constraints [15]. By toggling the electrometer between voltage (open-circuit) and current (short-circuit) mode, perturbations in the volume charge density
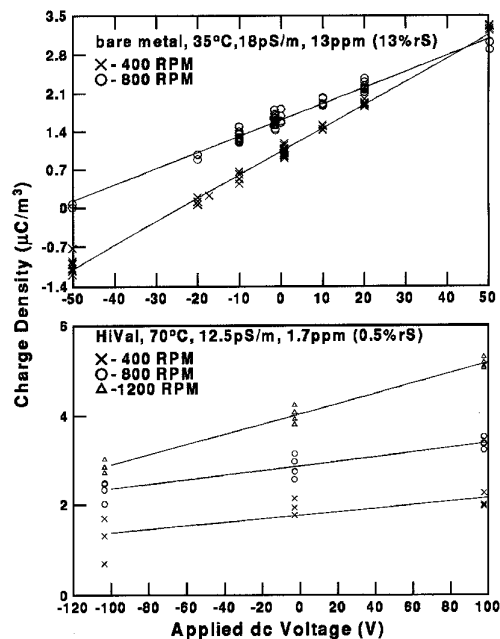

Figure 11. Charge density measurements with a dc voltage applied between the inner and outer cylinders. The inner cylinder rotation rate and oil properties are indicated. The upper plot had bare stainless steel cylinders while the lower plot had HiVal pressboard covering the inner cylinder. Different oil samples were used for each test. The solid lines indicate that the charge density increases linearly with applied voltage.

were observed, as shown in Figure 12. At the low rotation rates, when the terminal voltage and current were small, the charge density was unaffected by the terminal impedance. At the higher rotation rates, when the terminal current became appreciable, the short-circuit charge density was found to be smaller than the open-circuit charge density. These results are consistent with the applied voltage measurements showing the largest change in the charge density (with applied voltage) at the lowest rotation rates. When the applied voltage is large compared to the open-circuit voltage, as at low rotation rates, the perturbation in the charge density is larger than that observed by changing the load impedance, but when the applied voltage is small compared to the open-circuit voltage, as at high rotation rates, the charge density perturbation is also smaller. In general, accurate measurements of the change in the charge density with the terminal impedance were only obtained in this type of experiment; comparing sets of data where the rotation rate varied between open-circuit and short-circuit conditions usually showed similar trends, but small relative changes in the system temperature and oil conductivity obfuscated the results.

Transient measurements in which the charge density was measured after starting rotation and changing the terminal voltage provide insight into the charge transfer mechanism. The time transients in the core charge density were only measurable at the lower temperatures because the development times were longer
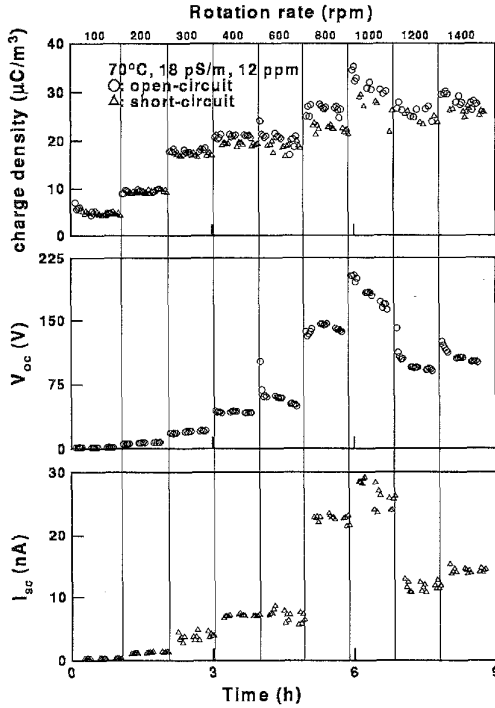
Figure 12. Charge density variation with terminal constraints for a copper sleeve covering the inner cylinder. This set of data shows the charge density being slightly larger when the terminals are open-circuited rather than short-circuited.

than the sampling time of the charge sensor. Representative transient measurements, shown in Figures 13 and 14 for a temperature of 15°C show that the charge density decreased immediately after applying a positive voltage and then decayed back to near its steady state level while the voltage was applied. The charge density increased when negative voltages were applied. The applied voltage did not appear to affect the steady state charge density appreciably, in contrast to the results of Figure 11, probably because the relative conductivity of the pressboard to the oil is very small at low temperatures [24].

One qualitative description of these transients comes from considering stationary cylinders so that the oil and pressboard can be described as simple dielectrics which have a single permittivity and conductivity. Electrically, the system can then be modeled as a Maxwell capacitor in cylindrical coordinates [25, pp. 184–188]. If the system starts from an uncharged state in which the interface between the oil and the pressboard is free of charge, then the application of a dc voltage between the electrodes will cause a current to flow through the system and a surface charge σ_f to develop on the interface according to

$$\sigma_f = \frac{\epsilon_2\sigma_1 - \epsilon_1\sigma_2}{\sigma_1 \ln(R_2/a) + \sigma_2 \ln(a/R_1)} \frac{V_o}{a} (1 - \exp[-t/\tau_c]) \quad (2)$$

with R_1 the inner cylinder radius, a the radius of the pressboard sleeve, $a - R_1$ the pressboard thickness, R_2 the outer cylinder radius, V_o the applied voltage, ϵ_1 the pressboard permittivity, σ_1
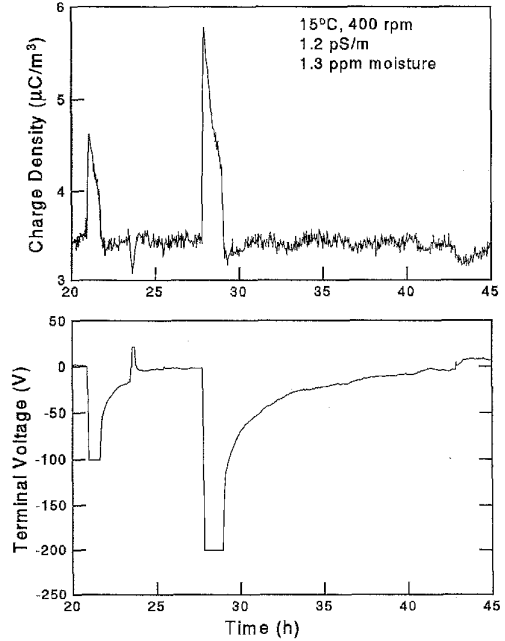

Figure 13. Transient voltage effect on the core charge density with HiVal pressboard covering the inner cylinder. The temperature was lowered (from 70°C) at time zero and the inner cylinder rotation was started at time 10.6 h and the terminals were short-circuited until 21 h. dc voltages of −100 V, 22.5 V, and −200 V were applied to the cylinders as shown. The open-circuit terminal voltage was measured when the voltage source was disconnected. The average pressboard moisture content was measured to be between 0.4 and 0.5%.

the pressboard conductivity, ϵ_2 the oil permittivity, σ_2 the oil conductivity, and τ_c the charging time constant given by

$$\tau_c = \frac{\epsilon_1 \ln(R_2/a) + \epsilon_2 \ln(a/R_1)}{\sigma_1 \ln(R_2/a) + \sigma_2 \ln(a/R_1)} \quad (3)$$

When the voltage source is disconnected, the decay of this surface charge depends upon the terminal connections. If the terminals are short-circuited by a current measuring electrometer, the current is the same through both the oil and the pressboard regions and the decay time is the same as the charging time constant τ_c. In contrast, if the terminals are open-circuited then the fields in each region decay independently so that there is no current flow through the terminals. The open-circuit voltage decay can be expressed as

$$v_{oc}(t) = v_1(0^-) \exp[-t/\tau_1] + v_2(0^-) \exp[-t/\tau_2] \quad (4)$$

where $v_1(0^-)$ is the initial voltage across the pressboard region, $v_2(0^-)$ is the initial voltage across the oil region, $\tau_1 \equiv \epsilon_1/\sigma_1$ is the pressboard dielectric relaxation time and $\tau_2 \equiv \epsilon_2/\sigma_2$ is the oil relaxation time. The first term reflects the decay of the field stored in the pressboard while the second term comes from the decay of the field across the oil. If a steady state had been achieved during the charging period ($t \gg \tau_c$), then the discharging transient becomes
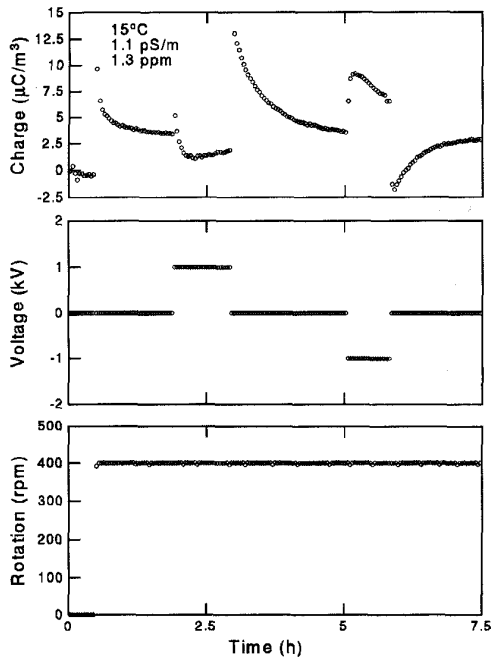
Figure 14. Voltage (± 1 kV) and rotation transient effects on the core charge density with HiVal pressboard covering the inner cylinder. This experiment used the same materials as those of Figure 13. The transients in the charge density appear to be consistent with the accumulation of surface charge at the pressboard/oil interface.

$$v_{oc}(t) =$$

$$V_o \left[\frac{\sigma_2 \ln(a/R_1) \exp[-t/\tau_1] + \sigma_1 \ln(R_2/a) \exp[-t/\tau_2]}{\sigma_1 \ln(R_2/a) + \sigma_2 \ln(a/R_1)} \right] \quad (5)$$

If the pressboard is much more insulating than the oil (so that the geometrical factors can be neglected), then the electrical energy is essentially stored in the field inside the pressboard and the free surface charge at the oil/pressboard interface is imaged to the inner cylinder. When the pressboard conductivity becomes comparable to the oil conductivity, more of the electric field passes through the oil and more of the free surface charge is imaged to the outer cylinder.

To explain qualitatively the experimentally observed transients in Figures 13 and 14, first assume that the effects of the applied voltage on the inner cylinder dominate those at the outer cylinder. To justify this assumption, note that the electric field is larger at the inner cylinder than the outer cylinder by the ratio of $R_2/a \approx 4/3$, the amount of charge taken from the inner cylinder sublayer is larger by the same ratio because the diffusion sublayer on the outer cylinder is larger by that ratio and less charge would be stripped away from the interface, and the inner cylinder surface area is smaller by the ratio a/R_2. The net contribution to the charge density should be higher from the inner cylinder by the ratio R_2/a and therefore only the charge dynamics near the inner cylinder interface will be discussed. Also, to be consistent with

the measured volume charge densities, assume that without rotation and without an applied voltage the chemically adsorbed surface charge on the inner cylinder is negative so that a positive volume charge density develops in the electrical double layer on the liquid side of the interface.

When the rotation of the inner cylinder is started, some of the positive volume charge is transported by the fluid into the core region. When a positive voltage is applied, the volume charge near the interface is decreased because negative volume charge accumulates to shield the applied field from the bulk of the fluid. This leads to a decrease in the core charge density as well. Because some of this negative charge gets adsorbed onto the interface to form a surface charge, the volume charge densities return to near their steady state levels. After removing the voltage source and keeping the terminals open-circuited (as in Figure 13), the accumulated surface charge leads to a terminal voltage that decays with the relaxation time of the pressboard. The charge density rapidly returns to its original level because the oil relaxation time is small compared to the charge density measurement time. In contrast, after removing the voltage source and keeping the terminals short-circuited (as in Figure 14), the accumulated negative surface charge is imaged by a positive volume charge on the liquid side of the interface and the core charge density then increases. When the surface charge decays, the core charge density also decays. The charging and discharging transients have similar time constants, consistent with the accumulation and decay of interfacial free surface charge discussed for ohmic dielectrics between stationary cylinders. The opposite polarity effect occurs when a negative voltage is applied.
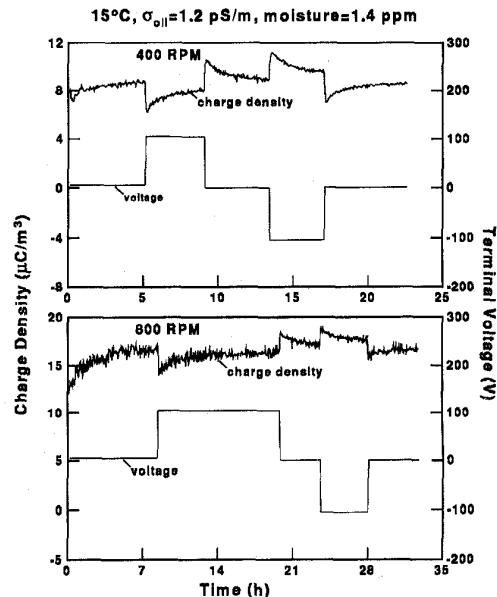

Figure 15. Voltage transient effects on the core charge density with HiVal pressboard covering the inner cylinder. Again, the transients in the charge density appear to be consistent with the accumulation of surface charge at the pressboard/oil interface.

A representative plot of the time transients in the charge density as the terminal voltage was varied for two rotation rates is given in Figure 15. By increasing the rotation rate, the diffusion sublayer thicknesses were decreased. Since the measured time constants associated with the transient decays in the charge densities were roughly the same at both rotation rates, the charge dynamics were probably reaction limited. In contrast, the charge density increased with rotation rate when there was no dc excitation, suggesting that the charge dynamics were at least partially transport limited. From these observations it would appear that the transport rate and the reaction rate for charge transfer at the interface are comparable for these semi-insulating materials.

3.6. CONDITIONING TRANSIENTS

While most of the measurements discussed thus far have focused on experiments that had a relatively short duration, long time transient variations were also observed in the experiments. In general terms, electrification (charge density, terminal current and voltage) measurements showed long time variations that were not correlated to measurements of the moisture content or conductivity. Since the electrification data is sensitive to the interfacial properties, it is concluded that the interfacial dynamics (adsorption and desorption of ions) are significant over these long transients.

One example of a 'conditioning' transient occurred with bare stainless steel cylinders. Initially, at temperatures of 15, 35, and 50°C, the charge density and terminal voltage had opposite polarities, but after reaching 70°C, they had the same polarity. Subsequent measurements showed that the charge density and voltage still had the same polarity, even at the lower temperatures. The terminal current tended to follow the voltage. These measurements indicate that the system was conditioned by some process. The terminal voltage showed the 'conditioning' process more markedly than the core charge density because it is more sensitive to differences in the interfacial properties [7]. One possible mechanism for the conditioning is that the different current densities at the cylinder interfaces led to the formation of oxide layers of different thicknesses. Indeed, related measurements of the leakage current as oil flows through a sintered filter have also shown passivation effects in which the current tends to decrease with time once the filter has come into contact with the fluid [26,27].

Another example of a conditioning transient, given in Figure 16, shows the charge density changing with a long time constant. During the initial equilibration period, the charge density appeared to vary inversely with the oil moisture content, but the charge density did not appear to follow the oil moisture content after that period; the moisture only appeared to be important during the initial phase. As in previous measurements, the low temperature charge density decreased as the conductivity increased. At the higher temperatures, the charge density did not consistently track with the conductivity. Thus, although the charge density occasionally tracked with the oil moisture and conductivity, the
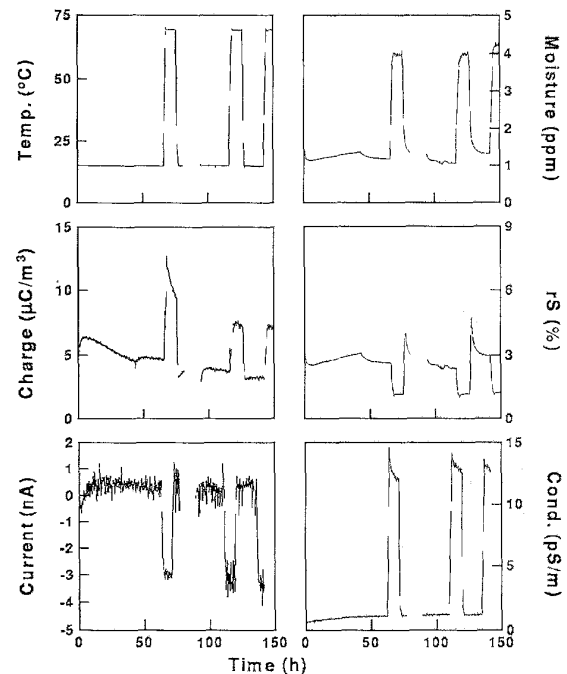

Figure 16. Conditioning transient during temperature cycling for HiVal pressboard covering the inner cylinder and 400 rpm. There was no rotation from 77 to 89 h. Initially the charge density appeared to vary inversely with the oil moisture content. After raising the temperature, the charge density followed the conductivity while the moisture remained constant. Repeated temperature cycling did not result in the sharp peak in charge density associated with the initial temperature transient increase.

long time transient change in the charge density was probably not caused by either of these.

Although relatively rare, the oil volume charge density was occasionally negative. Usually this resulted from long time transient changes in the system, but on one occasion, the charge density was negative immediately after the rotation was started. As shown in Figure 17, during the initial 15°C equilibration period, the moisture in the oil migrated into the pressboard and the oil conductivity remained essentially constant. On the other hand, the charge density was negative and the terminal current was positive and relatively large. During this period, sharp discontinuities in the charge density and current were present, which appear to be consistent with discharges in the system. Subsequent measurements showed the charge density and current repeatedly reversing polarity. Some of these polarity reversals were driven by changes in the temperature but others occurred at a constant temperature. In these extended measurements, the moisture content and conductivity increased slowly with time, indicating that the system was probably slightly exposed to the atmosphere.

One possible mechanism leading to the discharges is that surface charge was accumulating at the oil/pressboard interface as the fluid flow redistributed the charge in the system. Once enough surface charge accumulated, the associated electric field exceeded the local breakdown field which, in turn, caused all of
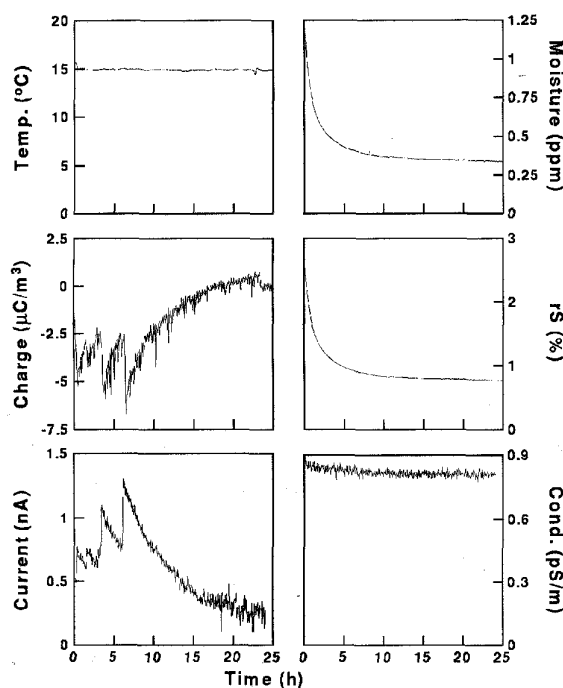
Figure 17. Initial 15°C equilibration period for HiVal pressboard covering the inner cylinder and 400 rpm. The oil moisture content slowly decreased as the pressboard dried the oil. The sharp discontinuities in the charge density and terminal current appear to be consistent with discharges in the system.

the accumulated charge to discharge. The discharge appeared to be global rather than local because the terminal current, which gives the net current flowing across the entire inner and outer cylinder interfaces, was discontinuous. The total charge involved in the discharge can be estimated from the discontinuity in the charge density and the volume of the annular gap. Using a volume of 6500 cm^3 and a charge density change of 4 $\mu C/m^3$, 26 nC of charge were discharged. With a rotational speed of 400 rpm corresponding to an average oil velocity of 190 cm/s (based on a radius of 9 cm), this quantity of charge is consistent with published magnitudes for electrostatic discharges created by flowing oils [28].

These results were somewhat surprising because discharges were not seen in previous or subsequent measurements. Although the oil moisture content was very low in this measurement, indicating that the pressboard insulation was also very dry, other experiments that achieved similar moisture contents did not exhibit these discharges. Furthermore, the change in the volume charge density as a result of the discharge was relatively small; other measurements showed larger volume charge densities at the same temperature, but no discharges. After disassembling the system and looking at the pressboard, the only surface blemish that was found was near the top of the inner cylinder. The blemish was slightly darker than the surrounding area and could have been due to the discharges. Apparently, once the local area of the discharge had been damaged, the discharges stopped.

In summary, these experiments highlight some of the difficulties associated with the electrification measurements. While numerous sets of experiments showed the same general trends (such as increased currents, voltages, and charge densities as the rotation rate or temperature were raised), there were also a number of experiments that exhibited longer time transient, conditioning behavior. Even though these experiments showed some of the nonreproducibility associated with the measurements, possibly due to leaks in the system or other uncontrolled parameters, they also showed long time scale dynamics. In a real transformer, both the initial conditioning phase, immediately after processing, and long time transient phases will be present. These measurements seem to indicate that the initial phase, immediately after processing, led to the largest electrification behavior.

3.7. EFFECTS OF COPPER

Since copper is present in large quantities in a transformer and deactivated by BTA [29], a thin sheet of copper was attached to the inner cylinder. Although the copper in a transformer is typically covered by paper or pressboard insulation, initial measurements were performed with bare copper on the inner cylinder. In general, copper and stainless steel appeared to have similar electrification characteristics. The system also went through the same type of conditioning transient observed with bare stainless steel cylinders in which the charge density and the terminal variables had opposite polarities at low temperatures, but after increasing the temperature to 70°C and then returning again to the lower temperatures, the charge density and terminal variables had the same polarity.

For comparison with earlier data without the copper, moisture and temperature transient measurements were also performed with HiVal pressboard insulation covering the copper sheet. For example, Figure 18, like Figure 7, shows the result of a step increase in temperature from 15 to 70°C. The moisture content tracked with the temperature and remained essentially constant once the temperature stabilized. The conductivity increased during the transient, then decreased slowly, even though the temperature was constant, possibly because of ionic absorption by the pressboard. The terminal current also decreased in magnitude, possibly as part of a conditioning phase in which the pressboard became more insulating with time. The charge density initially increased with the decreasing conductivity then remained essentially constant. Since a higher oil conductivity usually leads to a lower charge density, this suggests that another competing process canceled the effects of the oil conductivity on the charge density.

3.8. EFFECTS OF BTA

The effects of the additive BTA were measured during the transient period in which the BTA was added to the oil in the CF and also during relatively short duration measurements in which the
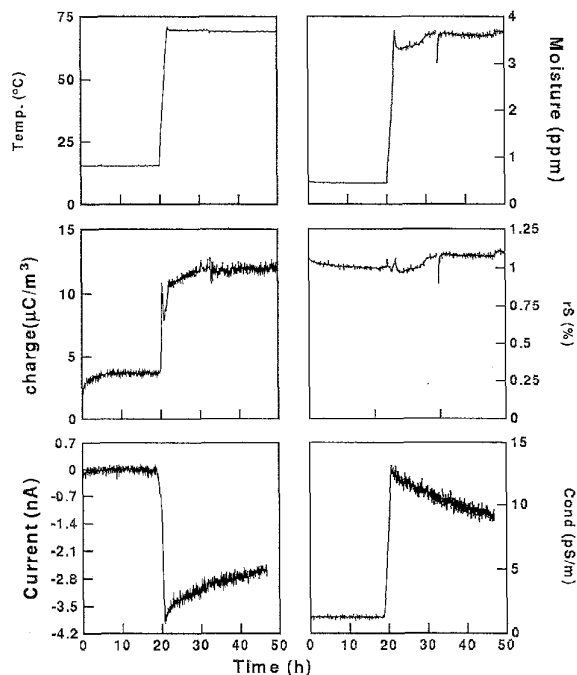
Figure 18. Initial temperature transient for HiVal pressboard covering the copper sleeve on the inner cylinder and 400 rpm. The step change in temperature drives the system to higher charge densities and terminal currents. Moisture is transferred out of the pressboard into the oil. The decrease in oil conductivity at the elevated temperatures is not completely understood; the terminal current followed the conductivity, but the charge density did not.

charge density, voltage, and current were measured as the rotation rate and temperature were varied. In addition to the electrification data, the oil moisture content and conductivity were monitored and the pressboard properties were inferred from periodic transient measurements of the open-circuit voltage and short-circuit current decays, just after disconnecting a dc voltage source or abruptly stopping the rotation of the inner cylinder. In the experiment discussed here, concentrated solutions of the BTA were periodically added to the oil, with the same oil and pressboard used throughout the experiment.

3.8.1. BTA MEASUREMENTS IN OIL

Before considering the effects of the BTA on electrification, first consider the mass transfer dynamics of the BTA in the oil. After adding the BTA to the oil in the CF, the BTA concentration slowly decreased, as shown in Figure 19 for several different initial BTA concentrations. This decrease in BTA concentration is similar to that observed in actual transformers [30].

Some of the concentration decrease can be attributed to the BTA absorption into the paper. Like any constituent present in trace amounts, the relative concentrations of the BTA in the oil and pressboard are determined by partition coefficients at each temperature. Although the details of the experiment were not provided the 'equilibrium' adsorption content of BTA in paper insulation has been given as 4.2 ppm of BTA (μg BTA/g pressboard)
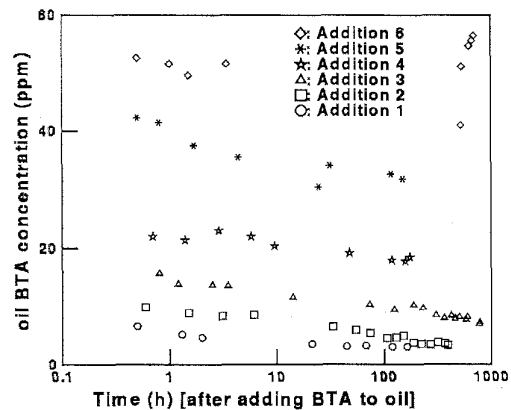

Figure 19. A series of measurements of the oil BTA concentration in the CC, which had a copper sheet over the inner cylinder, and HiVal pressboard over the copper sheet. Each symbol denotes a different initial BTA concentration. Throughout these transients, electrification measurements at numerous rotation rates and temperatures (15 to 70°C) were performed. The decrease in BTA concentration appeared to be independent of the temperature and flow conditions.

at 15°C and 21 ppm of BTA at 70°C [30]. Similar results have also been obtained by adding BTA to a beaker containing known masses of oil and paper insulation. By measuring the decrease in the oil BTA concentration and assuming that the concentration decrease was due to BTA migrating into the paper, the BTA concentration in the paper was calculated [31]. Since the BTA content of the oil was not reported, this would appear to be the solubility of BTA in the paper, but the measurements given in the next Section contradict this conclusion. For comparison, recall that the oil volume in the CC was $\sim$ 7500 cm^3 and the pressboard covering the inner cylinder only had a volume of $\sim$ 200 cm^3 so that only a small fraction of the BTA was expected to be transferred from the oil into the pressboard.

3.8.2. BTA MEASUREMENTS IN PRESSBOARD

Direct measurements of the BTA in the pressboard showed that significant amounts of BTA were present in the pressboard [15]. When the pressboard was diced, peeled, and mixed thoroughly with the extract solutions, the pressboard BTA concentration was estimated to be 130 ppm (μg BTA/g pressboard). The concentration was reasonably uniform over the height of the cylinder, being roughly 123 ppm at the top of the inner cylinder and 139 ppm BTA at the bottom. Additional measurements were performed to determine if the BTA was in the bulk of the pressboard or at the surface. In this case the pressboard samples were diced, but not peeled, and were mixed less thoroughly with the extract solutions to yield BTA concentrations of 67 ppm at the top of the inner cylinder, 62 ppm in the middle, and 59 ppm at the bottom. In the first set of measurements, the peeling of the pressboard increased the surface area exposed to the extract solution which, with the extra mixing, apparently allowed more of the BTA to be extracted from the pressboard. These results indicate that most of the BTA came from the bulk of the pressboard and not the surface. Otherwise,

the second set of measurements would have had BTA concentrations comparable to those of the first measurement. Based on these measurements, the solubility of the BTA in the pressboard is much higher than that given by the previously mentioned 'equilibrium' levels.

3.8.3. ELECTRIFICATION MEASUREMENTS

Consider next the transient when the concentrated solution of BTA was added to the oil in the CF, as shown in Figure 20. The measurements show that the BTA had both short term and long term effects. In the short term, immediately after adding the BTA, the charge density decreased and the current became positive and large. After this initial transient period, the charge density tended to be slightly enhanced and the current tended to become more negative. In the long term, the charge density and current were initially reduced when the BTA concentration was increased to ~ 10 ppm, but the magnitudes of the charge density and current were increased when the BTA concentration was increased further.

After the BTA concentrated oil was added, the oil was mixed for ~ 30 min before samples were withdrawn for BTA concentration measurements. The initial decay of the BTA was probably caused by the BTA being absorbed into the pressboard, but it could also have been an experimental artifact because the BTA had not yet been mixed uniformly into the oil of the CF or because the same 'T' port was used for both adding the BTA filled oil and withdrawing oil samples. The much slower decay of the BTA probably resulted from further absorption into the pressboard, adsorption onto the interfaces, or degradation of the BTA molecule itself, which is known to be light sensitive. These experiments were done with a minimal exposure to light, so that the degradation should have been minimal.

In these measurements, the oil moisture content remained essentially constant and only increased when the relatively 'wet' BTA concentrated oil (which contained ~ 15 ppm of water) was added to the system. The fact that the moisture content remained nearly constant indicates that the system was reasonably well sealed.

The BTA appeared to have a strong effect on the oil conductivity. This was a surprising result because BTA has been found to contribute little to the oil conductivity [28, 29] or to increase it [32], but those measurements showing an increased conductivity were performed with paraffinic oils rather than the naphthenic oil used here. One possible mechanism by which the BTA can reduce the conductivity of the oil is that the BTA molecules cluster around the ionic species, similar to the hydration of ions in water, thereby increasing the effective size and reducing the mobility of the ions. If the mobility is reduced enough, the clustering of the BTA around the ions could effectively reduce the number density of ions contributing to the conduction process. During the first addition, the conductivity increased probably as a result of the BTA concentrated oil having a high conductivity; in subsequent additions, the kettle containing the BTA concentrated oil, which was open to atmosphere, was raised to 70°C for much shorter periods

of time so that oil oxidation would be minimized. The significant increases in conductivity before the second and third additions of BTA may have been caused by the BTA concentrated oil not being degassed so that the oil could be oxidized more readily. The pressboard conductivity appeared to be unaffected by the BTA, but once the oil became very insulating, the pressboard appeared to become more insulating as well.

To help explain the role that the BTA played in reducing, and then enhancing, the electrification charge density, data were also obtained at various rotation rates and temperatures for experiments having a short duration compared to the decay in oil BTA concentration. The results are shown in Figure 21. During each measurement, the BTA concentration was essentially constant at the indicated levels.

At each BTA concentration, the charge density usually increased with both rotational speed and temperature, consistent with previous measurements. Similarly, the open-circuit voltage and short-circuit current tended to become larger in magnitude as the rotational speed and the temperature increased. Exceptions to this behavior occurred when the BTA concentration was near 5 to 10 ppm; the voltage then decreased as the rotation rate increased, in some cases, and the current occasionally reversed polarity. Measurements of the rate of change of the charge density with respect to the applied dc voltage show that both positive and negative values were obtained, but the scatter in the data prevents more detailed observations from being made.

The primary goal of this particular experiment was to determine the effect of the BTA on the electrification processes. These measurements showed that the addition of small concentrations of BTA, $\lesssim 10$ ppm, did not affect the electrification data significantly in charge density, voltage, and current. Once the oil contained $\gtrsim 10$ ppm of BTA, the magnitudes of the charge density, voltage and current were reduced. The electrification data remained at these reduced magnitudes even as the oil BTA concentration decayed. As more BTA was added, the charge density, voltage and current increased with BTA concentration. Subsequent measurements taken after the BTA had been in the system an additional 515 h showed that the electrification data again became smaller in magnitude. These measurements confirm some of the conclusions in the literature that an oil BTA concentration of about 10 ppm is critical for reducing the electrification [29, 33]. While polarity reversals or monotonic reductions in the electrification with increasing BTA concentrations were not observed, these effects may be caused by the differences in experimental configurations.

Physically, it appears that the BTA had two separate, but competing, effects on the electrification. As an illustration, represent the volume charge density on the liquid side of the solid/liquid interfaces with a wall charge density ρ_w. This wall charge density is assumed to be constant at a given temperature that is independent of rotational speed but dependent upon the BTA that has been added to the system. The first effect of the BTA was to reduce ρ_w, which reduces the charge in the interfacial electrical double layers and the magnitudes of the core charge density, voltage and
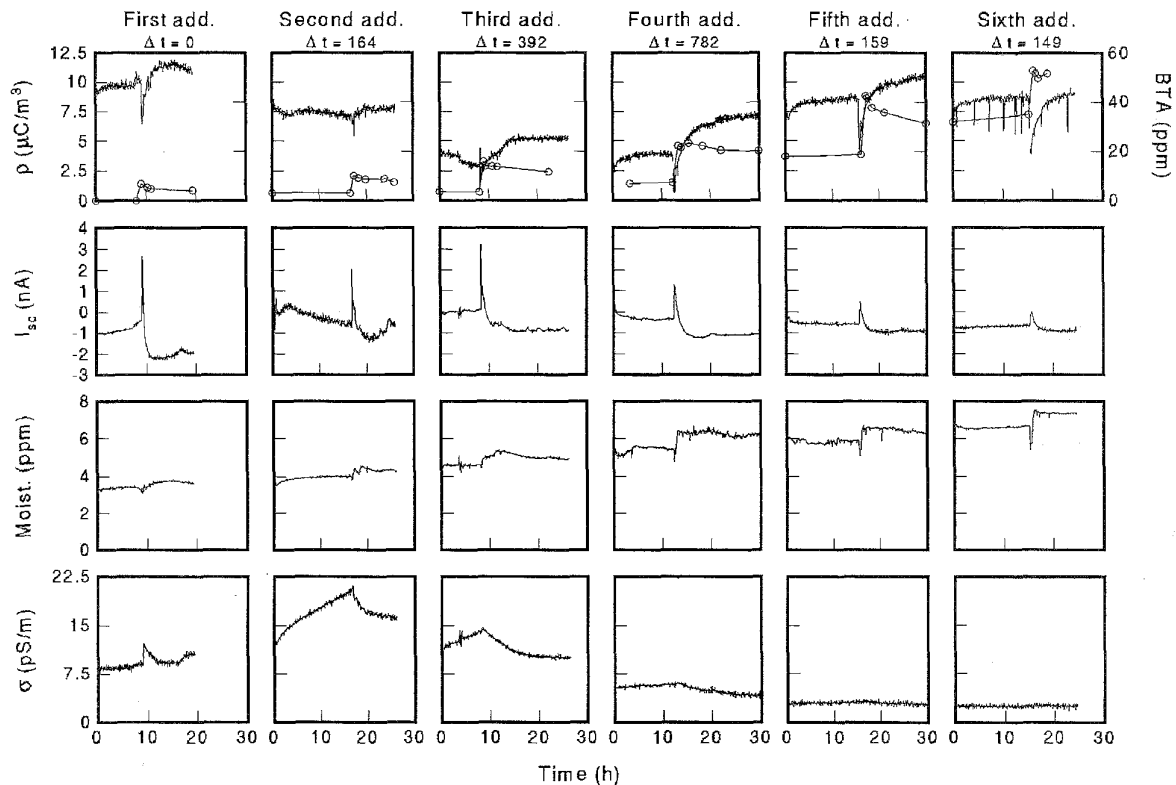
Figure 20. Time transient measurements associated with the addition of BTA to oil in the CF. The system was at 70°C with HiVal pressboard covering the copper sleeve on the inner cylinder and 400 rpm. Concentrated solutions of BTA in oil, also at 70°C, were added as indicated. The oil was periodically sampled and the BTA concentration, illustrated by the circles, measured using ultraviolet spectrophotometry. The time Δt (h) between additions of the BTA is indicated.

current. The second effect of the BTA was to reduce the oil conductivity, which tends to cause an increase in the core charge density. An exception to these effects is the data showing a decrease in the charge density as the oil conductivity increased; this increase in conductivity does not appear to be associated with the BTA and was probably the result of oil oxidation. In essence, the measurements are a superposition of the effects of the BTA reducing the wall charge density and the variations in the oil conductivity.

This physical model can also be used to describe qualitatively the time transient data when the BTA is added into the CF. On the short time scale, as the BTA is added to the oil, some of the BTA is immediately absorbed into the pressboard or, at least, onto the surface so that it can diffuse into the pressboard [33]. The BTA disrupts the diffuse charge distribution in the double layer, possibly by shielding the adsorbed interfacial surface charge. In the limit that all of the surface charge is shielded, then the wall charge density at the pressboard interface would become zero. The net effect is that the core charge density would also be reduced since charge would only be getting stripped away from the outer cylinder interface. Furthermore, the terminal current would become positive, assuming positive charge is diffusely distributed in the outer cylinder double layer, as positive charge is entrained in the

fluid flow and transported away from the outer cylinder interface. As the BTA diffuses into the bulk of the pressboard, less is present to shield the surface charge at the pressboard interface and the charge density and current return to their original levels. On the long time scale, as the BTA gets adsorbed onto the interface, the diffuse charge in the double layer is again reduced. Although somewhat speculative, this physical picture appears to be consistent with the essential features of the data.

4. COMPARISON TO CLASSICAL ELECTROCHEMISTRY

As discussed in the introduction, rotating cylindrical electrodes have been used to study mass transfer rates in aqueous electrolytic solutions. These studies typically use ionic salts which undergo a known chemical reaction with the electrode materials. Since the solutions typically have a conductivity on the order of 1 S/m, a net charge does not develop in the bulk of the liquid and the terminal (short-circuit) current is used to infer the chemical reaction rates at the inner cylinder. In general the current is affected by the transport of the ions to the interface and the interfacial chemical reaction. To reduce the effects of the transport so that only the reaction is being studied, supporting electrolytes are added which
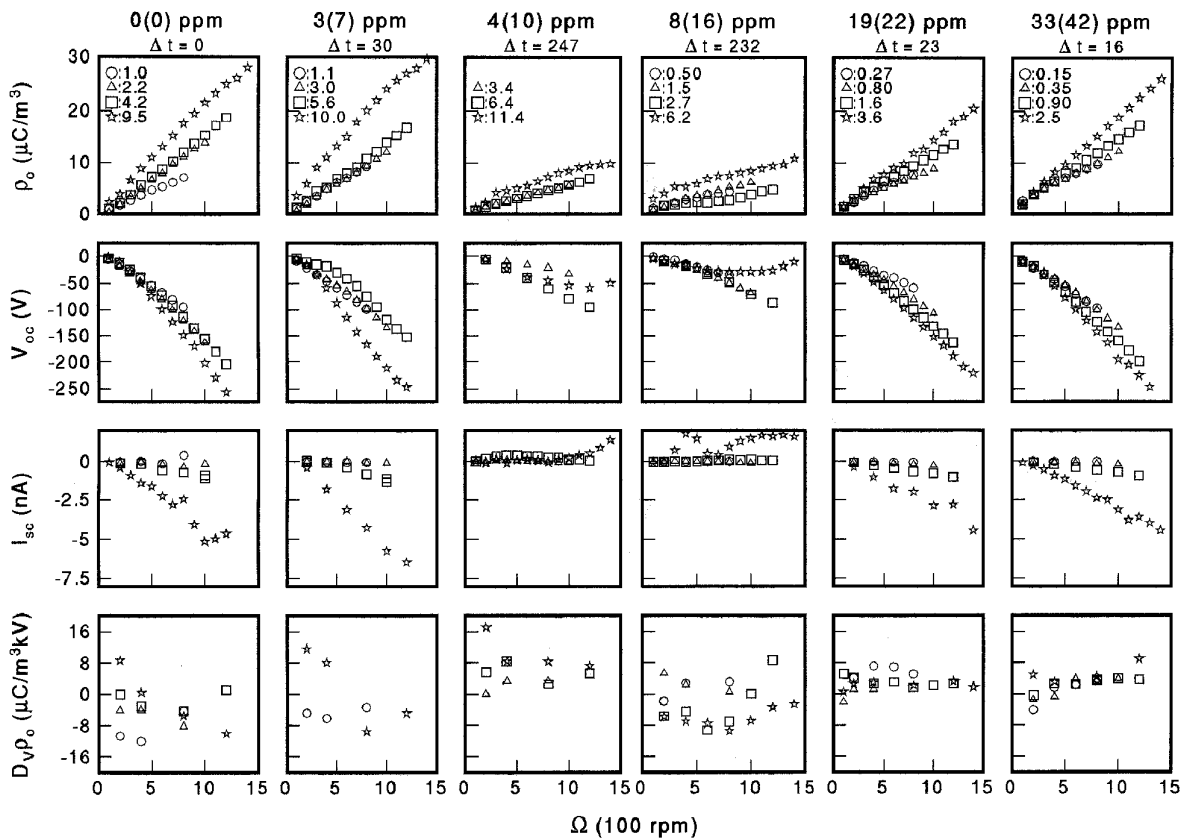
Figure 21. The steady state electrification data as the rotation rate of the inner cylinder, the temperature, and the BTA concentration are varied. The system had HiVal pressboard covering the copper sleeve on the inner cylinder. The oil BTA concentration during the reported measurements is given, with the number in parentheses denoting the initial measured concentration. The time Δt (h) between the current addition of BTA and the start of the set of electrification measurements is indicated. The symbols denote the temperature as circles:15°C, triangles:35°C, squares:50°C, and stars:70°C. The oil conductivity (pS/m) at each temperature is indicated.

raise the conductivity of the liquid but do not react at the interface. This reduces the electric field in the bulk of the solution so that the transport is essentially given by diffusion of the reacting species to the surface. By raising the rotational speed of the inner cylinder, the transport can be made fast compared to the reaction rates and the current is rate limited by the interfacial reactions. This is observed experimentally as a limiting current when the rotation rate is increased.

Extensive measurements have found that the nondimensional mass transfer rate, the Sherwood number S_h, is related to the drag coefficient C_f, Reynolds number R and Schmidt number S_c via

$$S_h \equiv \frac{2aJ_L}{zqc_oD_m} = \frac{C_f}{2}RS_c^{0.356} \qquad (6)$$

where J_L is the limiting current density at the inner cylinder, z is the valence of the reacting ion, q is the charge of a single electron, and c_o is the bulk concentration of the reacting species [34]. The drag coefficient can be expressed as

$$\frac{1}{\sqrt{C_f}} \approx -0.6 - 4.07\log_{10}\left(\frac{2}{R\sqrt{C_f}} + 0.215\frac{e}{a}\right) \qquad (7)$$
$$8 \times 10^2 < R < 8 \times 10^5$$

with e/a the surface roughness height divided by the inner cylinder radius [35]. Since the ionic species and concentrations in the Couette facility measurements are not known, the terminal current is converted into a Sherwood number using

$$S_h = \frac{Ib}{\pi H\sigma_2 D_m} = \frac{Iqz}{\pi H\sigma_2 kT} \qquad (8)$$

with H the cylinder height, σ_2 the oil conductivity, b the ionic mobility, D_m the molecular diffusivity of the ions, Boltzmann's constant $k = 1.38 \times 10^{-23}\ J/K = 8.6167 \times 10^{-5}$ eV/K, and T the temperature in Kelvin. The last equality uses Einstein's relation

$$\frac{D_m}{b} = \frac{kT}{qz} \qquad (9)$$

to relate the mobility and diffusivity. In this work the Schmidt number and Reynolds number are given by

$$S_c \equiv \frac{\nu}{D_m} \qquad R \equiv \frac{2\Omega a^2}{\nu} \qquad (10)$$

with Ω the cylinder angular velocity (rad/s) and ν the kinematic viscosity of the fluid, given by

$$\nu = \nu_o \exp[W_\nu/kT] \qquad (11)$$

where $\nu_o = 3.956 \times 10^{-10}$ m^2/s and $W_\nu = 0.2725$ eV [36]. Since the ionic species are not known, the ionic diffusivity must be estimated and a valence of $z = 1$ was assumed. Empirically, the ion mobility (SI unit m^2/Vs) in hydrocarbon liquids has been related to the viscosity (SI unit kg/s m) by Walden's rule as [37]

$$b\eta \approx 2 \times 10^{-11} \qquad (12)$$

with $\eta = \rho_m \nu$ the dynamic viscosity of the liquid and $\rho_m \approx 886$ kg/m^3 the oil mass density [38]. Thus, the temperature sets the viscosity of the oil and the ionic diffusivity can be estimated from the calculated mobility and the Einstein relation.
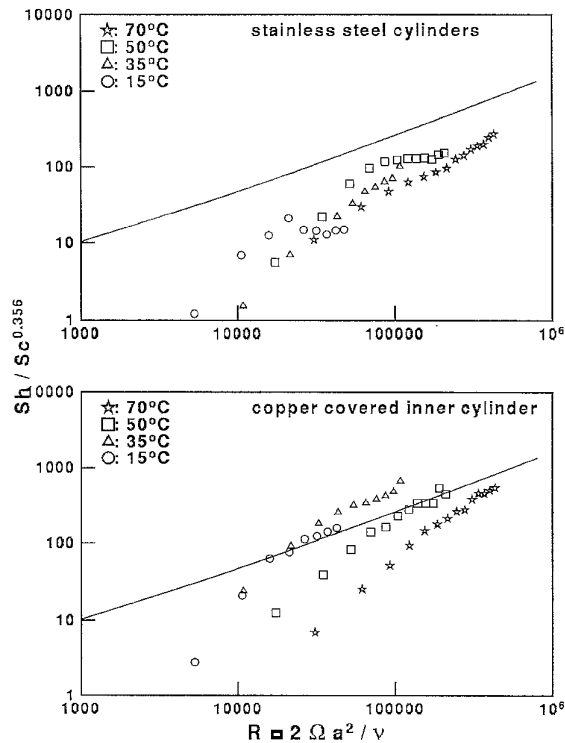

Figure 22. A comparison to classical electrochemical measurements for metal cylinders. The solid line represents the accepted current for reaction limited conditions (Equations (6) and (7) with $e/a = 0$).

Representative plots comparing the nondimensional current from the Couette facility to accepted correlations based on aqueous electrochemical measurements are given in Figures 22 and
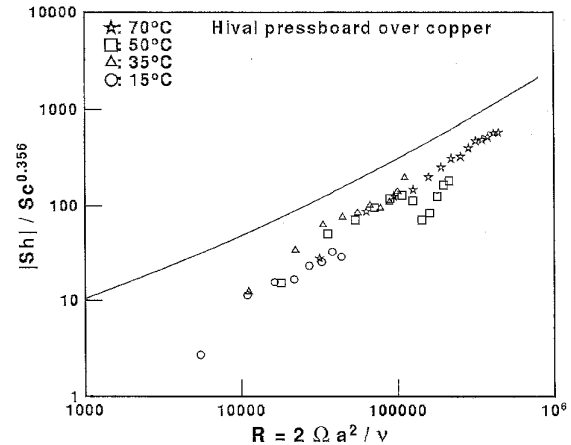

Figure 23. A comparison to electrochemical measurements for rough cylinders and HiVal pressboard covering the inner cylinder using the data of Figure 3. The solid line represents the accepted current for reaction limited conditions (Equations (6) and (7)), assuming a pressboard surface roughness of 100 μm [40] so that $e/a = 0.0013$.

23. In general, the Couette facility values are in good agreement with the accepted values. This is somewhat surprising because the ionic species are not known and estimates for the ionic diffusivity had to be used, the accepted correlations were found for lower Schmidt number fluids ($10 < S_c < 10^4$) as opposed to the $10^4 < S_c < 10^6$ range for transformer oil, and the current densities for the semi-insulating oils are much lower than those found in aqueous experiments (recall that the Sherwood number has the terminal current divided by the liquid conductivity). In light of these differences, the deviations of the experimental data from the accepted limiting current Sherwood numbers are not significant.

This data suggests that the transport of the ions to the interface and the reaction rates must be treated on equal footing. For low Reynolds numbers, the Couette facility Sherwood numbers are much lower than the reaction limited values. In contrast, at high Reynolds numbers the data approach a line that is roughly parallel to the reaction limited current. This indicates that the experiments span the transition from the transport limited regime to the reaction limited regime.

5. DISCUSSION

THIS paper presented a relatively extensive set of experimental measurements. While the data can be used on a purely empirical basis to determine how specific parameters affect the electrification processes, the data can also be compared to electrification models (in future papers) to explore some of the fundamental mechanisms for the interfacial charge transfer. The following summarizes the important observations from the experiments.

Measurements of the core charge density between rotating

cylindrical electrodes tended to show an increase with the rotation rate of the inner cylinder and with temperature. These measurements are similar to leakage current measurements in pipe flow experiments which show the leakage current becoming larger as the fluid velocity and the temperature increase. In addition, measurements of the terminal voltage and current between the cylinders usually track with the charge density, but occasionally they showed peaks at intermediate rotation rates and temperatures. Similarly, in transformers, measurements of the leakage current from the windings have shown peak magnitudes at intermediate temperatures.

Measurements of the charge density and terminal current at low oil moisture contents showed that the oil moisture content does not have a significant effect on the electrification processes. In contrast, the conduction through pressboard is strongly moisture dependent and decreasing the pressboard moisture content leads to less conduction and smaller terminal currents. An exception to the oil moisture dependence of the charge density was found during the initial equilibration period, immediately after processing of the pressboard, in which the oil was brought into contact with the pressboard. During this period, before the system was raised in temperature, the charge density appeared to vary inversely with the oil moisture content. This result seems to be consistent with ministatic tester measurements which show that the leakage current resulting from oil flowing through a paper filter increases as the oil moisture content decreases [36]. Furthermore, the charge density not appearing to change with the moisture content after the initial conditioning phase suggests that the ministatic tester measurements do not represent equilibrium measurements. Indeed, similar measurements with hydrocarbon liquids flowing through a filter required a conditioning phase in which the filter was immersed in the liquid being studied for a few hours or days before consistent and reproducible measurements were obtained [39]. Long time transients were also observed in experiments using an earlier version of the CF [4]. These conditioning transients, which had been associated with the oil and paper insulation coming to moisture equilibrium, were eliminated by heat treating and processing the paper. The processing was similar to the vacuum drying and oil impregnation of the pressboard performed in the experiments presented here. The difference in results may be due to the oil impregnation process happening more rapidly in the relatively thin paper, in the earlier measurements in the CF, vs. the thick pressboard used in these measurements.

Numerous measurements also showed that dc applied voltages, surface charge accumulation and terminal constraints, can affect the electrification charge density. In particular, while it is well known that energization itself, i.e. ac for power transformers, can enhance the charge density, measurements performed here showed that if the pressboard/oil interface accumulates charge from an external source and the source is then removed, the electrification charge density can then be increased or decreased, depending upon the polarity of the accumulated surface charge.

The terminal constraints (open or short-circuit) are also important in determining whether the electric field associated with the surface charge is through the pressboard or the oil; if the field is through the oil, the charge in the electrical double layer and the electrification charge density can be affected.

Copper was also added to the system to simulate the presence of copper in an actual transformer and the additive BTA tends to deactivate copper. Comparisons between the electrification data obtained with and without copper covering the stainless steel inner cylinder showed that the copper gave results similar to those with the stainless steel electrodes.

The effects of the additive 1,2,3 benzotriazole (BTA) were also studied. The BTA content of the oil in the Couette facility decayed with time, similar to that observed in actual transformers [28, 30], but on a different time scale. This confirms that the CF is a convenient facility for simulating at least the mass transfer dynamics in a full-scale transformer. The decrease in oil BTA content may be the result of the BTA being absorbed into the bulk of the pressboard, adsorbed onto the surfaces in the system, or even decomposition of the BTA molecule itself, which is known to be light sensitive. Direct measurements showed that significant amounts of BTA could be stored in the pressboard, but measurements of several standard solutions stored in amber high-density polyethylene bottles, in the absence of any light and pressboard, also showed concentration decreases. It is likely that all three factors contribute to the decrease in BTA concentration.

In regards to electrification, nominal BTA concentrations near 10 ppm appear to have caused a reduction in the magnitude of the electrification data. But the BTA also appeared to decrease the oil conductivity, which tends to increase the magnitude of the electrification data. These competing effects limit the effectiveness of the BTA, but over long periods of time the BTA appeared to cause a continual net decrease in the electrification charge density, possibly as a result of slow electrochemical adsorption of the BTA in the interfaces. These observations are consistent with some (but not all) of the literature describing the effects of BTA on electrification. For example, in some of the original experiments used as proof that BTA reduces the electrification charge density, the charge density decreased monotonically with increasing additive concentration (from a positive level toward zero) while other experiments taken over the same concentration range showed the charge density decreasing from a positive level, passing through zero, and becoming negative with a magnitude that increased with BTA concentration [28, 33]. Early laboratory measurements showed that the BTA had little [41] or no [36] effect on the electrification process, but subsequent measurements have shown that the BTA caused the charge density to become smaller or more negative [42] and long term effects caused a reversal in the charge density temperature dependence so that it decreased as the temperature increased [43].

Some of the experiments were also compared to established correlations from aqueous electrochemical measurements. The

data was in surprisingly good agreement with the established results, even though the liquid conductivities (and the resulting current densities) are roughly 12 orders of magnitude smaller and the charge carrying species are not known. This comparison also indicates that the electrification measurements are in a regime in which the charge transfer is transport limited at the lower Reynolds number flows, and rate limited at the higher Reynolds numbers.

ACKNOWLEDGMENT

REFERENCES

[1] V. G. Levich, *Physicochemical Hydrodynamics*, Prentice-Hall, New York, NY, 1962.

[2] D. R. Gabe, "The rotating cylinder electrode", Journal of Applied Electrochemistry, Vol. 4, pp. 91–108, 1974.

[3] D. R. Gabe and F. C. Walsh, "The rotating cylinder electrode: a review of development", Journal of Applied Electrochemistry, Vol. 13, pp. 3–22, 1983.

[4] D. J. Lyon, J. R. Melcher, and M. Zahn, "Couette charger for measurement of equilibrium and energization flow electrification parameters: application to transformer insulation", IEEE Transactions on Electrical Insulation, Vol. 23, No. 1, pp. 159–176, February 1988.

[5] J. Kedzia, "Measurement of the Electrification of Liquids in the Rotating Cylinder System", Journal of Electrostatics, Vol. 20, pp. 305–312, 1988.

[6] J. Kedzia, "Investigation of Transformer Oil Electrification in a Spinning Disk System", IEEE Transactions on Electrical Insulation, Vol. 24, No. 1, pp. 59–65, February 1989.

[7] A. J. Morin II, M. Zahn, and J. R. Melcher, "Fluid Electrification Measurements of Transformer Pressboard/Oil Insulation in a Couette Charger", IEEE Transactions on Electrical Insulation, Vol. 26, No. 5, pp. 870–901, 1991.

[8] R. M. Radwan, R. M. El-Dewieny, and I. A. Metwally, "Investigation of Static Electrification Phenomenon due to Transformer Oil Flow in Electric Power Apparatus", IEEE Transactions on Electrical Insulation, Vol. 27, No. 2, pp. 278–286, April 1992.

[9] J. Kedzia and B. Willner, "Electrification Current in the Spinning Disk System", IEEE Transactions on Dielectrics and Electrical Insulation, Vol. 1, No. 1, pp. 58–62, February 1994.

[10] P. K. Poovamma and R. Jagadish, "Influence of Surface Roughness and Thickness of Pressboard on the Charging Characteristics of Transformer Oil", Conference Record of the 1994 IEEE International Symposium on Electrical Insulation, June 1994, pp. 5–8.

[11] P. K. Poovamma, R. Jagadish, and K. Dwarakanath, "Investigation on static electrification characteristics of transformer oil", Journal of Electrostatics, Vol. 33, pp. 1–14, 1994.

[12] J. Rungis, R. G. Heydon, and A. Sierota, "Electrostatic Charging Tendency of Aged Transformer Oils", EPRI Workshop Proceedings; Static Electrification in Power Transformers, September 26–28, 1994.

[13] J. K. Nelson and M. J. Lee, "Tandem-chamber Charge Density Monitor", IEEE Transactions on Electrical Insulation, Vol. 25, No. 2, pp. 399–404, 1990.

[14] A. J. Morin II, M. Zahn, J. R. Melcher, and D. M. Otten, "An Absolute Charge Sensor for Fluid Electrification Measurements", IEEE Transactions on Electrical Insulation, Vol. 26, No. 2, pp. 181–199, 1991.

[15] A. P. Washabaugh, *Flow Induced Electrification of Liquid Insulated Systems*, ScD thesis, EECS Department, MIT, Cambridge, Mass., Dec. 1994.

[16] P. A. von Guggenberg and J. R. Melcher, "An Immersible Relative Saturation Moisture Sensor with Application to Transformer Oil", Proceedings of the 3rd International Conference on Properties and Applications of Dielectric Materials, July 1991, pp. 1258–1261.

[17] P. A. von Guggenberg, *Applications of Interdigital Dielectrometry to Moisture and Double Layer Measurements in Transformer Insulation*, PhD thesis, EECS Department, MIT, Cambridge, Mass., June 1993.

[18] E. T. Norris, HV Power Transformer Insulation", Proceedings IEE, Vol. 110, No. 2, Feb. 1963.

[19] A. P. Washabaugh and M. Zahn, "Flow Electrification Measurements in a Couette Flow Facility", IEEE International Symposium on Electrical Insulation, June 1994, Pittsburgh, PA.

[20] S. D. Foss, "Power Transformer Drying Model, Report DS-002–87", Technical Report, Dynamic Systems, Inc., Pittsfield, MA, October 1987, Prepared for the General Electric Company and the Consolidated Edison Corporation.

[21] A. P. Washabaugh and M. Zahn, "Flow Electrification Measurements in a Couette Flow Facility", Conference Record of the 1994 IEEE International Symposium on Electrical Insulation, June 1994.

[22] E. Brzostek and J. Kedzia, "Static Electrification in Aged Transformer Oil", IEEE Transactions on Electrical Insulation, Vol. 21, No. 4, pp. 609–612, August 1986.

[23] R. Tamura, Y. Miura, T. Watanabe, T. Ishii, N. Yamada, and T. Nitta, "Static electrification by forced oil flow in large power transformers", IEEE Trans. Power Apparatus and Systems, Vol. 99, No. 1, pp. 335–343, 1980.

[24] W. Kennedy, "Resistivity of oil and pressboard insulation and their effect on transformer design", EPRI Workshop Proceedings; Static Electrification in Power Transformers, June 1993, pp. 1-4-1–1-4-13, EPRI TR-102480.

[25] M. Zahn, *Electromagnetic Field Theory: a problem solving approach*, Reprint Edition, Kreiger, Malabar, Florida, 1987.

[26] R. G. Heydon, J. Rungis, and R. Sheehy, "The Use of Sintered Metal Filters in the Study of ECT in Transformer Oils", 1992 Annual Report, Conference on Electrical Insulation and Dielectric Phenomena, pp. 275–280, Oct. 1992.

[27] M. E. Furey, J. A. Palmer, and J. K. Nelson, "A New Reciprocating Apparatus for the Measurement of Electrostatic Charging Tendency of Transformer Oil", EPRI Workshop Proceedings; Static Electrification in Power Transformers, Sept. 28–30 1994.

[28] M. Ieda, T. Yanari, T. Miyamoto, and M. Higaki, "Investigation of Static Electrification in Large Power Transformers in Japan", EPRI Workshop Proceedings; Static Electrification in Power Transformers, June 1993, pp. 2-3-1–2-3-31, EPRI TR-102480.

[29] M. Yasuda, K. Goto, H. Okubo, T. Ishii, E. Mori, and M. Masunaga, "Suppression of Static Electrification of Insulating Oil for Large Power Transformers", IEEE Transactions on Power Apparatus and Systems, Vol. 101, No. 11, pp. 4272–4280, Nov. 1982.

[30] T. Miyamoto, A. Kishi, and Y. Miura, "Effect of Insulating Oils on Streaming Electrification in Transformer", EPRI Workshop Proceedings; Static Electrification in Power Transformers, July 1990, pp. 3-2-1–3-2-12, EPRI EL-6918.

[31] Personal communication with N. Hosokawa of the Mitsubishi Electric Corp. Sept. 1994.

[32] T. S. R. Murthy, Meenakshi, P. G. Agashe, and K. M. Kamath, "Studies of Electrostatic Charge Suppressants for Paraffinic Transformer Oils", 7th BEAMA International Electrical Insulation Conference, Brighton, England, May 23–26 1994.

[33] M. Ieda, K. Goto, H. Okubo, T. Miyamoto, H. Tsukioka, and Y. Kohna, "Suppression of static electrification of insulating oils for large power transformers", IEEE Transactions on Electrical Insulation, Vol. 23, No. 1, pp. 153–157, February 1988.

[34] R. Kappesser, I. Cornet, and R. Greif, "Mass Transfer to a Rough Rotating Cylinder", Journal of the Electrochemical Society, Vol. 118, No. 12, pp. 1957–1959, Dec. 1971.

[35] T. Theodorsen and A. Regier, "Experiments on drag of revolving disks, cylinders, and streamline rods at high speeds", Technical Report 793, NACA, 1944.

[36] T. V. Oommen, "Static Electrification Properties of Transformer Oil", IEEE Transactions on Electrical Insulation, Vol. 23, No. 1, pp. 123–128, Feb. 1988.

[37] I. Adamczewski, *Ionization, Conduction, and Breakdown In Dielectric Liquids*, Taylor and Francis, London, pp. 224–225, 1969.

[38] "Diala A oil, Diala AX oil: Electrical insulating oils for rapid heat transmission with high oxidation stability", Technical Bulletin SOC:39–85, Shell Oil Company, 1985.

[39] P. W. Huber and A. A. Sonin, "Electric Charging in Liquid Hydrocarbon Filtration: A Comparison of Theory and Experiments", Journal of Colloid and Interface Science, Vol. 61, No. 1, pp. 126–145, 1977.

[40] H. P. Moser, Ch. Krause, G. Praxl, G. Spandonis, R. Stonitsch, and H. Brechna, "Influence of Transformer Board and Nomex Board on the Electrification of Power Transformers", EPRI Workshop Proceedings; Static Electrification in Power Transformers, EPRI TR-102480, pp. 2-2-1–2-2-18, June 1993.

[41] D. W. Crofts, "Addition of 'BTA' to Transformer Oil for Control of Static Electrification", EPRI Workshop Proceedings; Static Electrification in Power Transformers, EPRI TR-102480. pp. 3-4-1–3-4-4, June 1993.

[42] P. J. Griffin and E. Finnan, "Assessment of Laboratory-Aged Insulating Materials using the Mini-Static Tester", EPRI Workshop Proceedings; Static Electrification in Power Transformers, September 26–28, 1994.

[43] M. A. Sens, J. B. Fernandez, and R. Ficara, "Benzotriazol Effects in Electrostatic Kraft Paper/Oil Flow Model Experiments", *EPRI Workshop Proceedings; Static Electrification in Power Transformers, September 26–28, 1994.*